JOURNAL OF PROTEOMICS 85 (2013) 129–159

Available online at www.sciencedirect.com

SciVerse ScienceDirect

www.elsevier.com/locate/jprot

The inducers 1,3-diaminopropane and spermidine cause the reprogramming of metabolism in *Penicillium chrysogenum*, leading to multiple vesicles and penicillin overproduction

Carlos García-Estrada[a,*], *Carlos Barreiro*[a], *Mohammad-Saeid Jami*[a], *Jorge Martín-González*[a], *Juan-Francisco Martín*[b,**]

[a]*INBIOTEC, Instituto de Biotecnología de León, Avda. Real no. 1, Parque Científico de León, 24006 León, Spain*
[b]*Área de Microbiología, Departamento de Biología Molecular, Universidad de León, Campus de Vegazana s/n; 24071 León, Spain*

ARTICLE INFO

Article history:
Received 21 February 2013
Accepted 15 April 2013
Available online 30 April 2013

Keywords:
1,3-diaminopropane
Spermidine
Penicillin
Penicillium chrysogenum
Vesicles

ABSTRACT

In this article we studied the differential protein abundance of *Penicillium chrysogenum* in response to either 1,3-diaminopropane (1,3-DAP) or spermidine, which behave as inducers of the penicillin production process. Proteins were resolved in 2-DE gels and identified by tandem MS spectrometry. Both inducers produced largely identical changes in the proteome, suggesting that they may be interconverted and act by the same mechanism. The addition of either 1,3-DAP or spermidine led to the overrepresentation of the last enzyme of the penicillin pathway, isopenicillin N acyltransferase (IAT). A modified form of the IAT protein was newly detected in the polyamine-supplemented cultures. Both inducers produced a rearrangement of the proteome resulting in an overrepresentation of enzymes involved in the biosynthesis of valine and other precursors (e.g. coenzyme A) of penicillin. Interestingly, two enzymes of the homogentisate pathway involved in the degradation of phenylacetic acid (a well-known precursor of benzylpenicillin) were reduced following the addition of either of these two inducers, allowing an increase of the phenylacetic acid availability. Both inducers produced also an increase in the intracellular content of vesicles that derived to vacuoles in late stages and promoted sporulation of *P. chrysogenum* in solid medium.

Biological significance
The analysis of global protein changes produced in response to polyamines 1,3-DAP and spermidine provides a valuable information for the understanding of the molecular mechanisms underlying the production of penicillin. This represents useful information to improve the production of this antibiotic and many other bioactive secondary metabolites not only in *P. chrysogenum*, but in other filamentous fungi as well.

* *Corresponding author*. Tel.: +34 987210308; fax: +34 987210388.
** *Corresponding author*. Tel.: +34 987291505; fax: +34 987291409.
E-mail addresses: c.gestrada@unileon.es (C. García-Estrada), jf.martin@unileon.es (J.-F. Martín).

1874-3919/$ – see front matter © 2013 Elsevier B.V. All rights reserved.
http://dx.doi.org/10.1016/j.jprot.2013.04.028

1. Introduction

The biosynthesis of penicillin in *Penicillium chrysogenum* is an excellent model to study the molecular mechanisms of biosynthesis, control of gene expression and secretion of secondary metabolites in fungi [1–3] due to the excellent knowledge accumulated on the biosynthesis [4,5] and molecular genetics of this β-lactam compound [3,6,7]. The penicillin biosynthetic pathway (Fig. 1) has been extensively reviewed [2–7]. Penicillin biosynthesis starts in the cytosol with the formation of the tripeptide δ-L-(α-aminoadipyl)-L-cysteinyl-D-valine (ACV) after the non-ribosomal condensation of L-α-aminoadipic acid, L-cysteine and L-valine. This reaction is catalyzed by the 426-kDa ACV synthetase (ACVS), which is encoded by the 11-kbp intron-free *pcbAB* gene. ACVS is synthesized as an inactive apoprotein that requires activation by means of the addition of a 4′-phosphopantetheine arm (derived from coenzyme A (CoA)) in a reaction carried out by a 4′-phosphopantetheinyl transferase (PPTase). During the next step, the oxidative ring closure of the tripeptide occurs, thus giving rise to the penam nucleus structure of isopenicillin N (IPN). This reaction takes place in the cytosol and is catalyzed by the 38-kDa IPN synthase or cyclase (encoded by the intronless *pcbC* gene). Once IPN is synthesized, it enters the peroxisome, where the L-α-aminoadipic side-chain of this intermediate is replaced by a hydrophobic acyl molecule. Side chain replacement is catalyzed by the peroxisomal acyl-CoA: IPN acyltransferase (IAT), which is encoded by the *penDE* gene. IAT is synthesized as a preprotein of 40 kDa termed proacyltransferase or proIAT. The proacyltransferase is autocatalytically self-processed into subunits α (11 kDa, corresponding to the N-terminal fragment) and β (29 kDa, corresponding to the C-terminal region), which constitute an active heterodimer. A two-step enzymatic process has been proposed for side chain replacement reaction. During the first step, the amidohydrolase activity removes the L-α-aminoadipate side chain of IPN, thus forming 6-aminopenicillanic acid (6-APA). Next, the acyl-CoA: 6-APA acyltransferase activity introduces the new activated acyl side chain. Activation of the precursor acyl molecules as CoA thioesters (phenylacetyl-CoA from phenylacetate in the case of benzylpenicillin) is a prerequisite for the incorporation of acyl side chains during the biosynthesis of hydrophobic penicillins and peroxisomal acyl-CoA ligases are in charge of such activation [2,3].

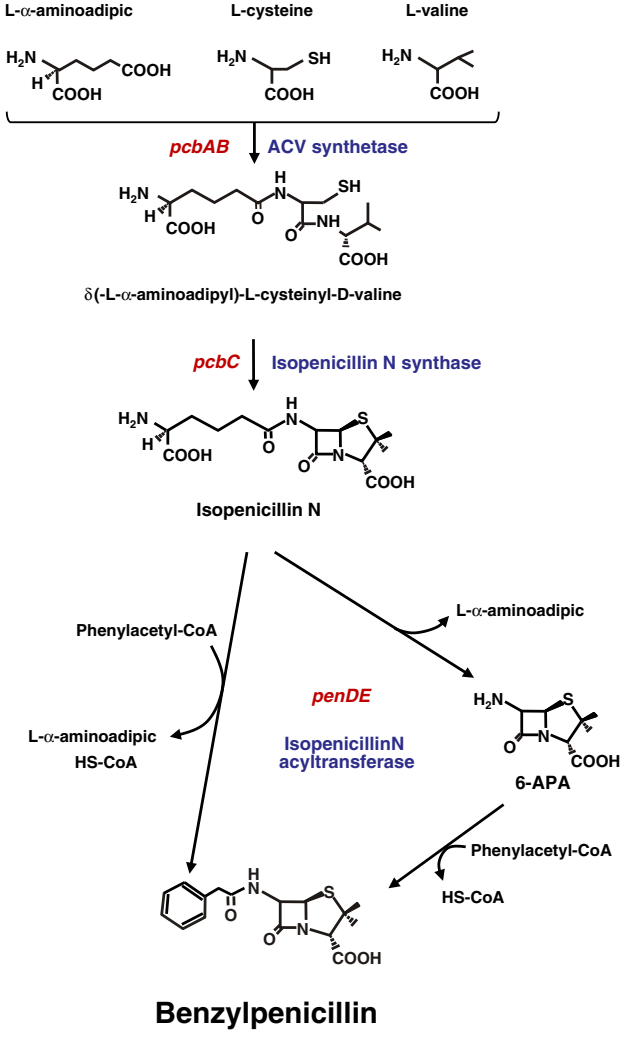

Fig. 1 – Schematic representation of the benzylpenicillin biosynthetic pathway.

The expression of the penicillin biosynthetic genes *pcbAB*, *pcbC* and *penDE* is greatly increased by the inducers 1,3-diaminopropane (1,3-DAP) and spermidine [8] that were initially identified in a screening of autoinducers synthesized by *P. chrysogenum* and *Acremonium chrysogenum* [9]. The inducing effect of 1,3-DAP and spermidine is not exerted by other diamines (e.g. putrescine, cadaverine or the triamine spermine), suggesting that the inducing effect is specific of those two compounds 1,3-DAP and spermidine that might be interconnected through conversion reactions. This induction is independent of the pH control mediated by the general pH regulator PacC. However, it appears to be mediated, at least partially, by the LaeA regulatory protein, since 1,3-DAP and spermidine restore the expression of penicillin biosynthesis genes and, therefore, penicillin production in a *laeA* defective mutant [8,10].

The stimulatory effect of 1,3-DAP and spermidine is observed not only on penicillin biosynthesis, but also on the formation of the green spore pigment and the brown mycelia pigment [8]. This effect is similar to that exerted by the LaeA regulatory protein both in *P. chrysogenum* [10] and in *Aspergillus nidulans* [11].

It is well known that the last two enzymes required for benzylpenicillin biosynthesis, namely phenylacetyl-CoA ligase (Phl) and isopenicillin N acyltransferase (IAT) are located in the peroxisome lumen [12–14]. Recent evidence in several filamentous fungi revealed an important role of endoplasmic reticulum (ER)-derived vesicles in the production of several secondary metabolites, including aflatoxins in *Aspergillus* species [15–17].

Proteomics is an interesting tool to study global protein changes in response to different inducers or stressing factors [18]. Proteomics has been applied to investigate changes in the proteome of *P. chrysogenum* during the strain improvement program [19,20]. Therefore, it was interesting to apply a combination of proteomics and other biochemical and microscopy tools to elucidate the role of 1,3-DAP on the shift of *P. chrysogenum* metabolism that leads to penicillin overproduction. In this article we report that both inducers

1,3-DAP and spermidine exert a strong effect on cellular metabolism resulting in a rearrangement of pathways for the synthesis of amino acids precursors of penicillin and an increase of the penicillin biosynthetic enzymes, in addition to the previously reported transcriptional activation of the penicillin biosynthetic genes *pcbAB*, *pcbC* and *penDE* [8]. Both inducers produce a significant increase of internal vesicles in the cytoplasm of the supplemented cells and also promote sporulation of *P. chrysogenum*.

2. Materials and methods

2.1. Strains and growth conditions

P. chrysogenum Wisconsin 54-1255 (reference laboratory strain for the genome sequencing project) was used in this work. For sporulation, Petri dishes containing solid Power medium [21] were initially sown with 1×10^8 spores from *P. chrysogenum* and were grown for six days at 25 °C. Conidia from one Petri dish were collected and inoculated into a flask with 100 ml of defined medium PMMY. It contains (g/l): $NaNO_3$ (3.0), yeast extract (2.0), NaCl (0.5), $MgSO_4 \cdot 7H_2O$ (0.5), $FeSO_4 \cdot 7H_2O$ (0.01) and glucose (40.0). For polyamine supplementation experiments, 5 mM of either 1,3-DAP or spermidine was added to the culture medium.

2.2. Protein samples preparation and 2-DE gel electrophoresis

Cultures were incubated in an orbital shaker for 48 h at 25 °C and 250 rpm and the mycelia was collected by filtration through a Nytal membrane, washed once with 0.9% NaCl, twice with double distilled water and stored at −80 °C. Frozen mycelia were ground to a fine powder in a precooled mortar using liquid nitrogen. Proteins were solubilized using phosphate buffer and precipitated with 2,2,2-tri-chloroacetic acid (TCA)/acetone as previously described [19]. The final pellet was washed twice with acetone followed by a final wash with 80% acetone and solubilized in 500 μl of sample buffer: 8 M urea, 2% (w/v) 3-[(3-cholamidopropyl)dimethylammonio]-1-propanesulfonate (CHAPS), 0.5% (v/v) ampholytes, 25 mM DTT and 0.002% bromophenol blue) and stored at −80 °C. The insoluble fraction was discarded by centrifugation at 13,200 rpm for 5 min. The supernatant was collected and the protein concentration was determined according to the Bradford method (Bio-Rad), which showed a high reproducibility for this protein extraction protocol.

A solution containing 350 μg of soluble proteins in the sample buffer (see above), was loaded onto 18-cm IPG strips (GE Healthcare), with non-linear (NL) pH 3–10 gradient. Focusing of proteins, equilibration of the focused IPG strips and the 12.5% SDS-PAGE for the second dimension (carried out in an Ettan Dalt Six apparatus (GE Healthcare)) were performed as previously described [19]. Gels were dyed with Colloidal Coomassie (CC) following the "Blue Silver" staining method [22].

2.3. Analysis of differential protein abundance

Scanned 2D gels were analyzed using an ImageScanner III (GE Healthcare) as described before [19]. Three biological replicates were used for each condition. Variability in the number of protein spots detected among biological replicates was less than 10%, which may be due to experimental variability. Spot normalization (internal calibration to make the data independent from experimental variations among gels) was made using relative volumes to quantify and compare the gel spots. Relative spot volumes correspond to the volume of each spot divided by the total volume of all the spots in the gel. Differentially expressed proteins between two conditions were considered when the ratio of the relative volume average for one specific spot (present in the three biological replicates) was higher than 1.5 and the p-value was <0.05.

2.4. Protein identification by tandem MS spectrometry

The protein spots of interest were manually excised, digested and processed as indicated before [19]. Samples were analyzed with a 4800 Proteomics Analyzer MALDI-TOF/TOF mass spectrometer (Applied Biosystems). A 4700 proteomics analyzer calibration mixture (Cal Mix 5; Applied Biosystems) was used as external calibration. All MS spectra were internally calibrated using known peptides from the trypsin digestion. The analysis by MALDI-TOF/TOF mass spectrometry produced peptide mass fingerprints, and the peptides observed (up to 65 peptides per spot) were collected and represented as a list of monoisotopic molecular weights with a signal to noise ratio greater than 20 using the 4000 Series Explorer v3.5.3 software (Applied Biosystems). All known contaminant ions (trypsin- and keratin-derived peptides) were excluded for later MS/MS analysis. From each MS spectra, the six most intensive precursors with a S/N greater than 20 were selected for MS/MS analyses with CID (atmospheric gas was used) in 2-kV ion reflector mode and precursor mass windows of ±7 Da. The default calibration was optimized for the MS/MS spectra.

Mascot Generic Files combining MS and MS/MS spectra were automatically created for protein identification, and used to interrogate a nonredundant protein database using a local license of Mascot v 2.2 from Matrix Science through the Protein Global Server (GPS) v 3.6 (Applied Biosystems). The search parameters for peptide mass fingerprints and tandem MS spectra obtained were set as follows: (i) NCBInr (2009.11.03) sequence databases were used; (ii) taxonomy: All entries (9993394 sequences, 3409286210 residues); (iii) fixed and variable modifications were considered (Cys as S carbamidomethyl derivative and Met as oxidized methionine); (iv) one missed cleavage site was allowed; (v) precursor tolerance was 100 ppm and MS/MS fragment tolerance was 0.3 Da; (vi) peptide charge: 1+; and (vii) the algorithm was set to use trypsin as the enzyme. Protein candidates produced by this combined peptide mass fingerprinting (PMF)/tandem MS search were considered valid when the global Mascot score was greater than 83 with a significance level of $p < 0.05$. Additional criteria for confident identification were that the protein match should have at least 15% sequence coverage; for a lower coverage, only those proteins with a Mascot ions score above 54 and at least two peptides identified in the tandem MS analysis (with a significance level of $p < 0.05$), were considered valid.

2.5. Analysis of the sporulation level

Spores were collected from Petri dishes sown with 1×10^8 spores of *P. chrysogenum* Wisconsin 54–1255 after six days of

incubation in the absence (control) or presence of either 1,3-DAP or spermidine, and counted. Those values provided by the control condition were set to 100. Results were provided as the mean plus standard deviation of three independent experiments carried out in triplicate. Data were subjected to one-way analysis of variance (ANOVA) and statistical significance was represented as "***" ($P \leq 0.001$).

2.6. *Scanning electron microscopy*

P. chrysogenum was grown on Power solid medium for six days at 28 °C in the absence and presence of either 5 mM 1,3-DAP or spermidine. Then, a portion of the sporulated solid medium from each condition was removed from the Petri dish, dried to a critical point using a dryer (BALZERS *CPD* 030), sputtered with 10 nm Au/Pd (BALZERS SCD 004) and examined with a JEOL 6100 scanning electron microscope.

3. Results

3.1. *Effect of 1,3-DAP on the intracellular proteome of P. chrysogenum*

It was previously reported that the addition of 1,3-DAP to pH-controlled fermentor cultures stimulate the biosynthesis of benzylpenicillin in *P. chrysogenum*, both in defined and in complex penicillin production media [8]. In order to provide a global vision about the biological mechanisms induced by 1,3-DAP, proteomics studies were conducted. Cultures of *P. chrysogenum* in the presence and absence of 1,3-DAP were performed and the intracellular protein fractions were analyzed by 2-DE and tandem MS spectrometry. The 2-DE gels obtained for both conditions were compared to each other (Fig. 2), showing 40 spots (including a total of 46 proteins) overrepresented and 27 spots (including 34 proteins) underrepresented after 1,3-DAP addition (Fig. 3). Proteins included in those spots were grouped according to functional categories (Tables 1 and 2) and the main findings are summarized below.

3.1.1. *Metabolism and energy*

There are some proteins directly related to the biosynthesis of penicillin and other secondary metabolites. Two proteins found overrepresented after the addition of 1,3-DAP are specially relevant. The first one is the IAT, which is involved in the last step of penicillin biosynthesis. One of the isoforms of this protein (spot Dc40) is only detected in the presence of the inducer (see Discussion) and this result correlates well with the observed increase in the penicillin titers after 1,3-DAP addition [8,9]. The second important protein, which is 3.28-fold overrepresented in the presence of 1,3-DAP, is a probable spermidine synthase Spe3 (spot Dc26). This finding is relevant, since 1,3-DAP is a by-product of spermidine degradation by the polyamine

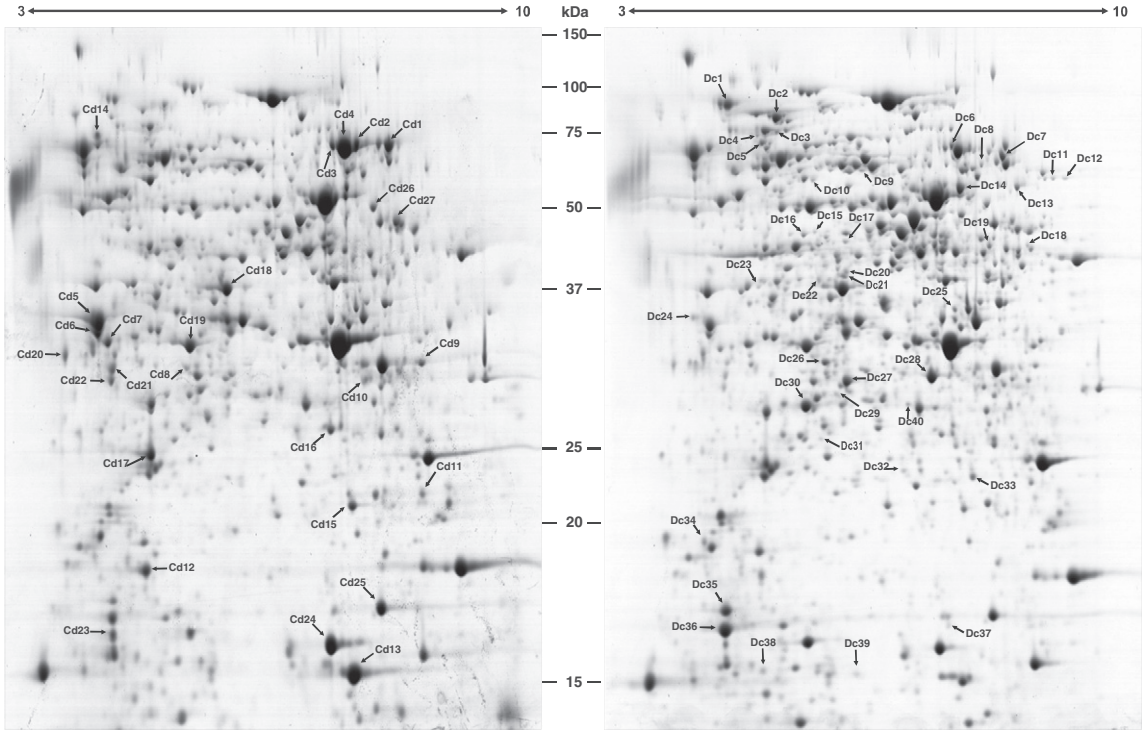

***P. chrysogenum* Wisconsin 54-1255. Intracellular proteome. Control**

***P. chrysogenum* Wisconsin 54-1255. Intracellular proteome. 1,3-DAP**

Fig. 2 – Comparison of the intracellular proteomes of *P. chrysogenum* Wisconsin 54-1255 with or without the addition of 1,3-DAP. 2-DE gels of the intracellular proteomes of the Wisconsin 54-1255 strain grown for 40 h in the absence (control) or presence of 1,3-DAP. The designation "Cd" is used for those spots underrepresented after the addition of this polyamine, whereas "Dc" is used for those spots overrepresented after treatment with 1,3-DAP. The spots differentially represented are numbered and correspond to those proteins listed in Tables 1 and 2.

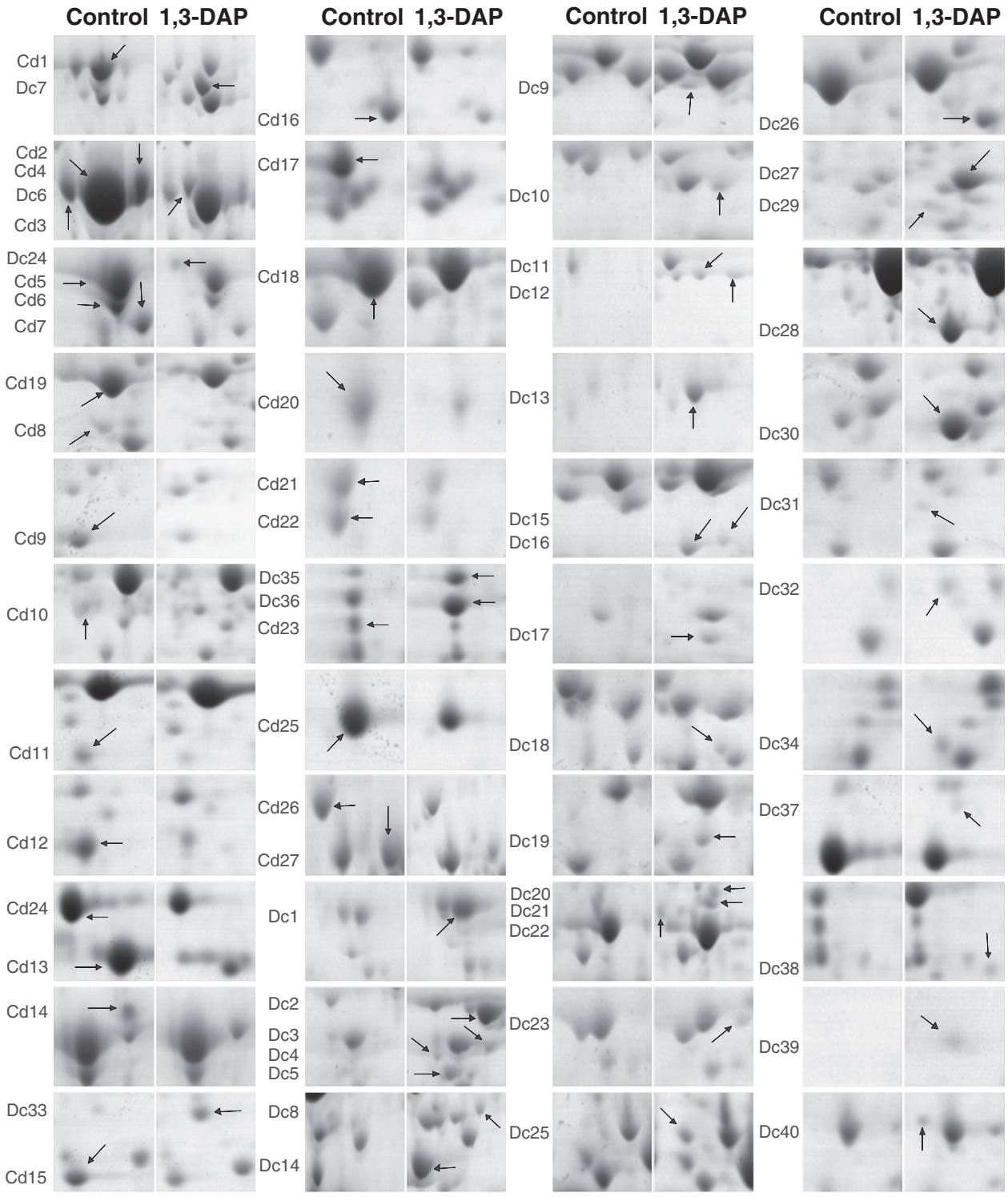

Fig. 3 – Close-up view of the spots differentially represented after addition of 1,3-DAP. Enlargement of gel portions containing the spots overrepresented in the gels of Fig. 2. The designation "Cd" is used for those spots underrepresented after the addition of this polyamine, whereas "Dc" is used for those spots overrepresented after treatment with 1,3-DAP. The spots differentially represented are numbered and correspond to those proteins listed in Tables 1 and 2.

oxidase (see Discussion) and there might be a direct conversion of 1,3-DAP into the three-carbon propylamino moiety of spermidine.

Another interesting enzyme only detected under 1,3-DAP supplementation conditions is a probable UTP-glucose-1-phosphate uridylyltransferase Ugp1 (spot Dc8). This enzyme, also known as UDP-glucose pyrophosphorylase, catalyzes the interconversion between MgUTP + glucose-1-phosphate and UDP-glucose + MgPPi and in addition to its role in glycogenesis, it has been suggested to be essential for the completion

Table 1 – Proteins overrepresented in the *P. chrysogenum* Wisconsin 54-1255 intracellular proteome after the addition of 1,3-DAP. Fold increase and p-value are indicated for those proteins detected under both conditions. Proteins that are only detected after the addition of 1,3-DAP are denoted as N/A.

Spot	ORF name	Accession no.	Title	Theoretical		Estimated								
				Mass (kDa)	pI	Mass (kDa)	pI	Peptides identified	Un-matched peptides	Score	Percent coverage (%)	Fold increase	p-value	Function
Metabolism and energy														
Dc6	Pc21g01110	gi|255952859	Strong similarity to 3-methylcrotonyl-CoA carboxylase (MCC) non-biotin-containing beta subunit like protein An07g04270 — *Aspergillus niger*	62.6	7.7	64.7	7.1	19	41	683	44	N/A	N/A	Leucine metabolism
Dc7	Pc18g05320	gi|211587092	Strong similarity to IMP dehydrogenase IMH3 — *Candida albicans*	57.9	6.5	60.3	7.8	17	46	696	45	3.46	4.28E−04	Purine metabolism
Dc8	Pc21g12790	gi|211590017	Strong similarity to UTP-glucose-1-phosphate uridylyltransferase Ugp1 — *Saccharomyces cerevisiae*	57.7	6.4	59.1	7.5	19	46	552	51	N/A	N/A	Glycogenesis
Dc11	Pc12g03370	gi|211581841	Strong similarity to mitochondrial F1-ATPase alpha-subunit Atp1 — *Saccharomyces cerevisiae*	59.8	9.0	55.1	8.4	18	19	614	39	N/A	N/A	ATP biosynthesis
Dc12	Pc12g03370	gi|211581841	Strong similarity to mitochondrial F1-ATPase alpha-subunit Atp1 — *Saccharomyces cerevisiae*	59.8	9.0	55.1	8.6	22	32	575	43	N/A	N/A	ATP biosynthesis
Dc13	Pc21g17880	gi|211590494	Strong similarity to 4-aminobutyrate transaminase gatA — *Aspergillus nidulans*	55.2	8.8	53.6	8.0	27	33	693	72	2.75	2.75E−04	β-alanine biosynthesis
Dc14	Pc20g04720	gi|211587749	Strong similarity to precursor of dihydrolipoamide dehydrogenase Lpd1 — *Saccharomyces cerevisiae*	54.6	7.7	51.7	7.3	30	29	999	64	2.05	6.95E−06	Acetyl-CoA biosynthesis
Dc16	Pc21g01100	gi|255952857	Strong similarity to isovaleryl-coenzyme A dehydrogenase like protein An07g04280 — *Aspergillus niger*	47.0	5.8	43.2	5.2	25	39	745	63	2.91	3.06E−04	Leucine metabolism
Dc17	Pc18g02760	gi|211586850	Strong similarity to hypothetical aldehyde dehydrogenase CAB63554.1 — *Schizosaccharomyces pombe*	54.2	5.5	42.8	5.8	17	48	712	46	N/A	N/A	b-alanine biosynthesis
Dc18	Pc21g20480	gi|255956565	Strong similarity to ATP citrate lyase ACL1 — *Sordaria macrospora*	71.9	7.6	42.3	8.1	15	48	784	27	N/A	N/A	Acetyl-CoA biosynthesis
Dc19	Pc21g20480	gi|255956565	Strong similarity to ATP citrate lyase ACL1 — *Sordaria macrospora*	71.9	7.6	42.1	7.6	20	44	657	31	N/A	N/A	Acetyl-CoA biosynthesis
Dc20	Pc18g02760	gi|211586850	Strong similarity to hypothetical aldehyde dehydrogenase CAB63554.1 — *Schizosaccharomyces pombe*	54.2	5.5	38.5	5.8	19	46	731	47	N/A	N/A	b-alanine biosynthesis

Dc21	Pc18g02760	gi|211586850	Strong similarity to hypothetical aldehyde dehydrogenase CAB63554.1 — *Schizosaccharomyces pombe*	54.2	5.5	37.9	5.8	17	43	786	46	N/A	N/A	b-alanine biosynthesis
Dc22	Pc18g02760	gi|211586850	Strong similarity to hypothetical aldehyde dehydrogenase CAB63554.1 — *Schizosaccharomyces pombe*	54.2	5.5	37.4	5.4	10	38	401	32	N/A	N/A	b-alanine biosynthesis
Dc23	Pc20g11650	gi|255945767	Strong similarity to bifunctional purine synthase like protein An15g00570 — *Aspergillus niger*	85.1	5.3	36.6	4.7	4	10	259	9	N/A	N/A	Purine metabolism
Dc25	Pc20g01610	gi|211587455	Strong similarity to mitochondrial malate dehydrogenase Mdh1 — *Saccharomyces cerevisiae*	36	8.4	34.5	7.2	16	12	1030	62	N/A	N/A	Krebs cycle
Dc26	Pc13g12400	gi|211584276	Strong similarity to spermidine synthase Spe3 — *Saccharomyces cerevisiae*	33	5.5	30.4	5.5	11	54	413	40	3.28	8.89E−04	Polyamine metabolism
Dc30	Pc12g00830	gi|211581603	Strong similarity to sorbitol utilization protein *sou2* — *Candida albicans*	29	5.3	27.4	5.2	17	47	531	80	6.10	6.33E−07	Carbohydrate metabolism
Dc37	Pc22g10040	gi|211592030	Strong similarity to glucosamine-6-phosphate deaminase like protein An16g09070 — *Aspergillus niger*	40	6.1	14.8	7.1	7	23	368	36	N/A	N/A	Aminosugar metabolism
Dc40	Pc13g08270	gi|211583872	Adenylylsulfate kinase AAA81521 — *Penicillium chrysogenum*	24	6.0	27.1	6.6	12	53	321	72	N/A	N/A	Purine, seleno amino acids and sulfur metabolism
	Pc21g21370	gi|211590823	Acyl-coenzyme A:isopenicillin N acyltransferase (acyltransferase) AAT/PenDE — *Penicillium chrysogenum*	40	6.2	27.1	6.6	11	54	281	37	N/A	N/A	Penicillin biosynthesis
Information pathways															
Dc2	Pc22g19990	gi|211592918	Strong similarity to endonuclease SceI 75 kDa subunit Ens1 — *Saccharomyces cerevisiae*	72.6	5.6	80.5	4.9	28	34	769	49	4.39	5.32E−04	Protein fate
Dc3	Pc22g10220	gi|211592047	Strong similarity to dnaK-type molecular chaperone Ssb2 — *Saccharomyces cerevisiae*	67.0	5.3	69.7	4.9	11	54	232	31	N/A	N/A	Protein fate
Dc4	Pc22g10220	gi|211592047	Strong similarity to dnaK-type molecular chaperone Ssb2 — *Saccharomyces cerevisiae*	67.0	5.3	68.5	4.6	20	44	705	47	N/A	N/A	Protein fate
Dc5	Pc22g10220	gi|211592047	Strong similarity to dnaK-type molecular chaperone Ssb2 — *Saccharomyces cerevisiae*	67.0	5.3	65.8	4.7	25	38	1060	50	4.70	1.25E−04	Protein fate
Dc10	Pc15g00640	gi|211584913	Strong similarity to GDP dissociation inhibitor in the secretory pathway Gdi1 — *Saccharomyces cerevisiae*	52.1	5.3	54.6	5.4	19	46	293	54	N/A	N/A	Protein fate
Dc24	Pc13g08810	gi|211583926	Strong similarity to elongation factor 1beta EF-1 — *Oryctolagus cuniculus*	25.0	4.4	33.9	3.8	8	41	748	59	N/A	N/A	Protein synthesis

(continued on next page)

Table 1 (*continued*)

Spot	ORF name	Accession no.	Title	Theoretical		Estimated								
				Mass (kDa)	pI	Mass (kDa)	pI	Peptides identified	Un-matched peptides	Score	Percent coverage (%)	Fold increase	p-value	Function
Information pathways														
Dc31	Pc16g01190	gi|211585160	Strong similarity to actin-binding protein like protein An03g06960 — *Aspergillus niger*	84	4.9	24.8	5.5	11	14	462	20	N/A	N/A	Protein with binding function or cofactor requirement
Dc32	Pc18g00860	gi|255942327	Weak similarity to suppressor of tom1 protein Mpt4 — *Saccharomyces cerevisiae*	34.5	9.7	22.7	6.5	9	36	143	28	N/A	N/A	Protein synthesis
Dc33	Pc18g00860	gi|255942327	Weak similarity to suppressor of tom1 protein Mpt4 — *Saccharomyces cerevisiae*	34.5	9.7	22.6	7.4	11	50	347	30	4.30	4.59E−04	Protein synthesis
Dc34	Pc21g03140	gi|211589089	Strong similarity to cell cycle regulator p21 protein wos2p — *Schizosaccharomyces pombe*	22	4.5	18.6	4.0	9	54	203	39	N/A	N/A	Cell cycle and DNA processing
Dc36	Pc20g13270	gi|211588542	Strong similarity to nascent polypeptide-associated complex alpha chain alpha-NAC — *Mus musculus*	22	4.7	14.8	4.2	3	62	88	20	2.64	2.04E−05	Transcription
Dc38	Pc22g16880	gi|211592618	Strong similarity to steroid membrane binding protein like protein An04g00560 — *Aspergillus niger*	14	5.1	13.1	4.7	8	48	464	80	N/A	N/A	Protein with binding function or cofactor requirement
Cellular transport and transport routes														
Dc3	Pc21g15100	gi|211590231	Strong similarity to H+-transporting ATPase vma-1 — *Neurospora crassa*	66.6	5.2	69.7	4.9	23	42	483	49	N/A	N/A	Proton transport
Dc9	Pc22g13480	gi|211592291	Strong similarity to vacuolar H(+)-transporting ATPase subunit B Vma2 — *Saccharomyces cerevisiae*	56.1	5.7	57.6	6.0	22	39	788	55	N/A	N/A	Proton transport

Perception and response to stimuli															
Dc8	Pc16g13280	gi|211586250	Strong similarity to glutathione reductase Glr1 — *Saccharomyces cerevisiae*	51.5	6.2	59.1	7.5	11	54	338	33	N/A	N/A	Cell rescue, defense and virulence
Dc10	Pc22g01020	gi|255946760	Strong similarity to choline sulfatase betC — *Sinorhizobium meliloti*	66.5	5.7	54.6	5.4	22	40	653	53	N/A	N/A	Cell rescue, defense and virulence
Dc35	Pc22g23760	gi|211593284	Strong similarity to type 2 peroxiredoxin like protein An12g08570 — *Aspergillus niger*	19	4.9	15.5	4.2	12	53	752	68	3.24	3.74E−05	Cell rescue, defense and virulence
Developmental processes															
Dc1	Pc22g09380	gi|211591967	Strong similarity to glycosylphosphatidylinositol-anchored beta(1–3) glucanosyltransferase gel3 — *Aspergillus fumigatus*	57.6	4.9	82.4	4.2	11	36	427	24	3.51	3.54E−04	Biogenesis of cellular components
Dc15	Pc20g11630	gi|211588384	Gamma-actin act-*Penicillium chrysogenum*	41.8	5.5	44.4	5.4	5	17	343	17	N/A	N/A	Biogenesis of cellular components
Other proteins															
Dc22	Pc22g04410	gi|211591496	Strong similarity to Ngg1p-interacting factor Nif3 — *Saccharomyces cerevisiae*	38.8	5.4	37.4	5.4	7	44	242	31	N/A	N/A	Unknown
Dc27	Pc21g12310	gi|255955019	Hypothetical protein [*Penicillium chrysogenum*]	30.4	5.6	28.9	5.8	18	38	505	67	3.03	3.52E−04	Unknown
Dc28	Pc12g08070	gi|211582258	Weak similarity to hypothetical protein Ta1372 — *Thermoplasma acidophilum*	27	5.0	28.8	6.9	13	49	418	61	N/A	N/A	Unknown
Dc29	Pc12g08070	gi|211582258	Weak similarity to hypothetical protein Ta1372 — *Thermoplasma acidophilum*	27	5.0	27.8	5.7	4	18	222	25	N/A	N/A	Unknown
Dc36		gi|144952798	16 kDa allergen [*Penicillium chrysogenum*]	16	5.2	14.8	4.2	4	61	404	21	2.64	2.04E−05	Unknown
Dc39	Pc20g07680	gi|255945047	Strong similarity to hypothetical protein contig1487_1.tfa_820cg — *Aspergillus fumigatus*	16.3	9.1	13.0	5.9	5	35	314	40	N/A	N/A	Unknown

Table 2 – Proteins underrepresented in the *P. chrysogenum* Wisconsin 54-1255 intracellular proteome after the addition of 1,3-DAP. Fold decrease and p-value are indicated for those proteins detected under both conditions. Proteins that are not detected after the addition of 1,3-DAP are denoted as N/A.

Spot	ORF name	Accession no.	Title	Theoretical		Estimated								
				Mass (kDa)	pI	Mass (kDa)	pI	Peptides identified	Un-matched peptides	Score	Percent coverage (%)	Fold decrease	p-value	Function
Information pathways														
Cd5	Pc22g11240	gi|211592088	Strong similarity to heat shock protein 70 *hsp70* — *Ajellomyces capsulatus*	69.7	5.03	32.9	4.0	18	47	586	39	2.92	7.03E−04	Protein fate
Cd6	Pc22g11240	gi|211592088	Strong similarity to heat shock protein 70 *hsp70* — *Ajellomyces capsulatus*	69.7	5.03	32.1	4.0	15	46	469	32	3.16	1.11E−03	Protein fate
Cd7	Pc22g19990	gi|211592918	Strong similarity to endonuclease SceI 75 kDa subunit Ens1 — *Saccharomyces cerevisiae*	72.6	5.58	31.4	4.1	19	46	438	27	3.44	1.33E−04	Protein fate
Cd9	Pc21g02360	gi|211589011	Strong similarity to GU4 nucleic-binding protein 1 Arc1 — *Saccharomyces cerevisiae*	47.8	6.4	29.8	8.3	13	36	662	40	2.50	7.53E−04	Protein with binding function or cofactor requirement
Cd11	Pc21g11890	gi|255954935	Strong similarity to RNA binding protein 47 RBP47 — *Nicotiana plumbaginifolia*	44.0	6.00	20.9	8.3	10	42	387	35	3.17	1.90E−04	Protein with binding function or cofactor requirement
Cd14	Pc22g02800	gi|61380693	Calreticulin [*Penicillium chrysogenum*]. strong similarity to calcium-binding protein precursor cnx1p — *Schizosaccharomyces pombe*	61.8	4.78	67.4	4.0	10	55	324	22	N/A	N/A	Protein fate
	Pc21g11280	gi|211589871	Strong similarity to protein disulfide isomerase A pdiA — *Aspergillus niger*	57	4.7	67.4	4.0	11	54	222	28	N/A	N/A	Protein fate
Cd17	Pc20g11850	gi|211588406	Strong similarity to elongation factor 1-gamma 1 Tef3 — *Saccharomyces cerevisiae*	46	5.8	23.3	4.7	7	58	112	24	2.01	1.22E−05	Protein synthesis
Cd20	Pc12g10670	gi|255932663	Strong similarity to dnaK-type molecular chaperone *bipA* — *Aspergillus niger*	73.7	4.81	30.4	3.6	8	22	477	14	2.10	4.11E−06	Protein fate
Cd21	Pc22g11240	gi|211592088	Strong similarity to heat shock protein 70 *hsp70* — *Ajellomyces capsulatus*	69.7	5.03	29.3	4.2	16	46	562	33	3.20	3.07E−03	Protein fate
Cd22	Pc22g11240	gi|211592088	Strong similarity to heat shock protein 70 *hsp70* — *Ajellomyces capsulatus*	69.7	5.03	28.4	4.2	14	51	428	29	2.27	1.31E−03	Protein fate
Cd23	Pc21g03140	gi|211589089	Strong similarity to cell cycle regulator p21 protein wos2p — *Schizosaccharomyces pombe*	22	4.5	14.1	4.2	10	55	315	39	2.31	7.76E−03	Cell cycle and DNA processing
Cd25	Pc16g13060	gi|211586228	Strong similarity to cyclophilin cypB — *Aspergillus nidulans*	18	6.9	15.1	7.7	8	57	408	44	2.03	3.50E−04	Protein fate
Perception and response to stimuli														
Cd2	Pc12g03130	gi|211581818	Strong similarity to acetyl-CoA hydrolase Ach1 — *Saccharomyces cerevisiae*	58.3	6.17	63.4	7.4	23	42	697	63	5.61	7.78E−05	Cell rescue, defense and virulence
Cd3	Pc12g03130	gi|211581818	Strong similarity to acetyl-CoA hydrolase Ach1 — *Saccharomyces cerevisiae*	58.3	6.17	63.4	7.1	26	35	746	63	3.31	3.43E−03	Cell rescue, defense and virulence
Cd4	Pc12g03130	gi|211581818	Strong similarity to acetyl-CoA hydrolase Ach1 — *Saccharomyces cerevisiae*	58.3	6.17	62.0	7.2	22	42	758	63	3.57	4.05E−07	Cell rescue, defense and virulence
Cd8	Pc12g09030	gi|255932349	Strong similarity to fumarylacetoacetase — *Homo sapiens*	46.6	6.01	29.4	5.2	12	53	297	31	2.53	1.89E−04	Homogentisate pathway

Cd12	Pc12g09030	gi|255932349	Strong similarity to fumarylacetoacetase — *Homo sapiens*	46.6	6.01	16.8	4.6	6	14	320	22	3.41	6.73E−06	Homogentisate pathway
Cd16	Pc12g09020	gi|255932347	Strong similarity to maleylacetoacetate isomerase *maiA* — *Aspergillus nidulans*	24.9	6.45	25.0	7.0	18	47	667	84	2.73	1.41E−03	Homogentisate pathway
Cd19	Pc12g09030	gi|255932349	Strong similarity to fumarylacetoacetase — *Homo sapiens*	46.6	6.01	31.0	5.2	14	50	560	40	2.13	9.09E−04	Homogentisate pathway
Cd24	Pc21g16940	gi|255955883	Strong similarity to Cu,Zn superoxide dismutase *sodC* — *Aspergillus fumigatus*	16.0	5.94	13.6	7.1	11	54	562	88	2.12	1.77E−03	Cell rescue, defense and virulence
Metabolism and energy															
Cd1	Pc22g03660	gi|211591424	Strong similarity to isocitrate lyase *acuD* — *Aspergillus nidulans*	60.1	6.52	63.0	7.8	19	28	523	49	3.98	1.04E−05	Glyoxylate and dicarboxilate metabolism
Cd10	Pc06g01600	gi|255930411	Strong similarity to FAD dependent L-sorbose dehydrogenase SDH — *Gluconobacter oxydans*	65.3	6.1	28.5	7.5	11	54	288	28	2.55	2.82E−04	L-ascorbic acid synthesis
	Pc22g10040	gi|211592030	Strong similarity to glucosamine-6-phosphate deaminase like protein An16g09070 — *Aspergillus niger*	40	6.1	28.5	7.5	10	55	133	43	2.55	2.82E−04	Aminosugar metabolism
	Pc12g06870	gi|211582144	Strong similarity to succinyl coenzyme A synthase alpha subunit SYRTSA — *Rattus norvegicus*	35	8.9	28.5	7.5	8	57	123	31	2.55	2.82E−04	Krebs cycle
	Pc12g04650	gi|211581953	Strong similarity to purine-nucleoside phosphorylase — *Bos taurus*	33	5.9	28.5	7.5	7	58	98	35	2.55	2.82E−04	Purine metabolism
Cd26	Pc16g07470	gi|211585695	Strong similarity to glycine decarboxylase subunit T Gcv1 — *Saccharomyces cerevisiae*	52	8.9	47.6	7.6	24	39	953	64	2.19	2.13E−04	Glycine to 5,10 methylene tetrahydrofolate catabolism
Cd27	Pc20g13510	gi|211588565	Strong similarity to methylcitrate synthase *mcsA* — *Aspergillus nidulans*	51	8.4	45.2	7.9	23	40	645	59	4.01	1.55E−04	Propionate to pyruvate oxidation through methylcitrate cycle
Cellular transport and transport routes															
Cd17	Pc20g04810	gi|211587757	Strong similarity to estrogen receptor-binding cyclophilin *cypD* — *Bos primigenius taurus*	41	5.9	23.3	4.7	10	55	478	37	2.01	1.22E−05	Component of the mitochondrial permeability transition pore
Other proteins															
Cd8	Pc22g09910	gi|255948466	Strong similarity to hypothetical protein SPAC1F3.09 — *Schizosaccharomyces pombe*	64.5	5.71	29.4	5.2	13	52	115	29	2.53	1.89E−04	Unknown
Cd13	Pc12g00650	gi|211581586	Similarity to hypothetical protein CC3092 — *Caulobacter crescentus*	15	6.1	12.5	7.4	12	53	811	95	3.45	2.16E−04	Unknown
Cd15	Pc23g00350	gi|255951667	Hypothetical protein BAC82546 — *Penicillium chrysogenum*	22.5	6.05	20.2	7.3	11	54	605	47	2.33	4.30E−04	Unknown
	Pc24g02750	gi|34392437	Hypothetical protein [*Penicillium chrysogenum*]	23.2	5.58	20.2	7.3	9	56	442	36	2.33	4.30E−04	Unknown
Cd18	Pc21g02210	gi|211588997	Strong similarity to hypothetical protein contig31_part_ii.tfa_2190wg — *Aspergillus fumigatus*	35	5.6	33.1	5.9	6	4	489	23	2.23	1.58E−06	Unknown

of development of the slime mold *Dictyostelium discoideum* [23–25], probably through its contribution to the cell wall biosynthesis.

Acetyl-CoA is a precursor of the α-aminoadipic acid side chain of penicillin. The biosynthesis of acetyl-CoA seems to be favored after 1,3-DAP addition. Mechanisms for the production of acetyl-CoA are represented by a probable ATP citrate lyase ACL1 (spots Dc18 and Dc19, only detected under supplementation conditions) and a probable mitochondrial precursor of dihydrolipoamide dehydrogenase Lpd1 (spot Dc14, 2.05-fold overrepresented). Indeed, the homocitrate synthase enzyme that introduces acetyl-CoA to the α-aminoadipic acid biosynthetic route has been reported to be a mitochondrial enzyme [26,27]. Production of ATP is also favored by 1,3-DAP, since two isoforms of a probable mitochondrial F1-ATP synthase alpha-subunit ATP1 (spots Dc11 and Dc12) are only detected under induction conditions. The ATP synthase complex consists of two major components, soluble F1 (containing the catalytic core) and membrane-bound F0 [28]. It has been observed that although the ATP1 protein is essential for mitochondrial ATP synthase function, it is not essential for life in yeast and deletion of ATP1 leads to a "petite" phenotype that is slow-growing but still able to survive on fermentable carbon sources [29].

It is also interesting to note that four isoforms of a hypothetical aldehyde dehydrogenase are only detected after the induction with 1,3-DAP (spots Dc17, Dc20, Dc21 and Dc22). This enzyme shows high similarity with aldehyde dehydrogenases from different ascomycetes (i.e. 95% similarity and 87% identity with the ALD3 from *Neosartorya fischeri*). It has been reported that the ALD2 and ALD3-encoding genes are required for β-alanine (3-aminopropionic acid) biosynthesis in *Saccharomyces cerevisiae* [30]. Related to these results is the overrepresentation (2.75 times) of a probable 4-aminobutyrate transaminase (spot Dc13). The latter is involved in the conversion of 4-aminobutanoate (GABA) + 2-oxoglutarate to succinate semialdehyde + L-glutamate and participates in β-alanine metabolism. These two enzymes are ω-aminotransferases acting on ω-aldehydes. Biochemical studies using purified enzymes of *P. chrysogenum* showed that those enzymes are essential for the conversion of α-aminoadipic semialdehyde into lysine and vice versa [31] (see Discussion).

An adenylylsulfate kinase AAA81521 (only detected under inducing conditions; spot Dc40) participates in sulphur metabolism catalyzing the synthesis of activated phosphoadenylylsulfate. The latter is a key step in the conversion of sulfate into SH2 and cysteine, which is precursor of the ACV tripeptide giving rise to penicillin.

3.1.2. *Information pathways*

Some proteins differentially represented after the addition of 1,3-DAP are involved in protein fate mechanisms (see Discussion). Treatment with 1,3-DAP induces the biosynthesis of i) three isoforms of a probable DnaK-type molecular chaperone Ssb2 (spots Dc3, Dc4 and Dc5), ii) Gdi1, a probable GDP dissociation inhibitor in the secretory pathway (spot Dc10), which plays an essential function in membrane traffic and in the recycling of proteins of the Sec4/Ypt/rab family from their target membranes back to their vesicular pools [32] and iii) one isoform of a probable 75 kDa subunit Ens1 endonuclease SceI (spot Dc2), which is a mitochondrial version of the 70-kDa heat shock protein (HSP70) [33]. Although 1,3-DAP induces the biosynthesis of those chaperones, this compound seems to exert a stronger effect leading to a reduction in the biosynthesis of several well-known chaperones and foldases (see Table 2).

Transcription and translation activating factors are also affected by 1,3-DAP. One interesting information-pathways protein that is overrepresented after 1,3-DAP addition is a probable suppressor of tom1, protein Mpt4. This protein, found in spots Dc32 (only detected under 1,3-DAP supplementation) and Dc33 (4.30-fold overrepresented), is a ribosome-associated protein from *S. cerevisiae* required for optimal translation under nutrient stress [34]. Indeed, penicillin production follows carbon and phosphate limitation stress [35]. Under these nutrient limitation conditions the Mpt4 protein may keep the translation of penicillin biosynthetic enzymes active for prolonged time, as observed previously [8]. A probable nascent polypeptide-associated complex alpha chain alpha-NAC (spot Dc36), which has been reported to function as a transcriptional coactivator [36], is 2.64-fold overrepresented under these conditions.

3.1.3. *Cellular transport, transport facilitation and transport routes*

The addition of 1,3-DAP seems to increase the generation of proton gradient across membranes, since two subunits of the vacuolar H^+-transporting ATPase were detected only after the addition of 1,3-DAP (spots Dc3 and Dc9). Vacuolar ATPases acidify several intracellular organelles and pump protons across the plasma membranes of numerous cell types (see Discussion).

On the contrary, 1,3-DAP decreases the biosynthesis of a probable estrogen receptor-binding cyclophilin CypD (spot Cd17). This protein has been found to play an important role in the mitochondrial permeability transition, in which mitochondrial pores open, leading to cell death in mammals [37,38].

3.1.4. *Response to stimuli*

Two proteins overrepresented after 1,3-DAP addition are involved in cell redox homeostasis. A probable type 2 peroxiredoxin like protein is found 3.24-fold overrepresented (spot Dc35), whereas a probable glutathione reductase Glr1 is only detected under 1,3-DAP supplementation (spot Dc8). The latter has been found as one of the proteins overrepresented in the penicillin high-producer strain AS-P-78 [19]. This enzyme probably plays a role in maintaining the ACV tripeptide in the reduced monomer (ACV-SH) form, which is required for penicillin biosynthesis [39]. Another interesting finding is present in spot Dc10. This spot is only detected after 1,3-DAP addition and includes a probable choline sulfatase BetC, which is involved in the conversion of choline-O-sulfate and, at a lower rate, phosphorylcholine, into choline. Choline is the precursor for glycine betaine, which is a potent osmoprotectant accumulated by *Sinorhizobium meliloti* to cope with osmotic stress [40]. The osmotic stress produced by the very dense culture medium in industrial fermentations may require compensating concentrations of glycine betaine.

Underrepresented proteins after the addition of 1,3-DAP are also found in this response to stimuli category of proteins. It is striking that two of these proteins belong to the

phenylacetate degradation homogentisate pathway. Three isoforms of a probable fumarylacetoacetase are found in spots Cd8, Cd12 and Cd19. This enzyme catalyzes the hydrolytic cleavage of a carbon–carbon bond in fumarylacetoacetate to yield fumarate and acetoacetate as the final step in phenylacetate, phenylalanine and tyrosine degradation [41]. The other enzyme from the homogentisate pathway is a probable maleylacetoacetate isomerase, which is 2.73-fold underrepresented (spot Cd16) in the presence of 1,3-DAP. This enzyme is also involved in tyrosine and phenylalanine catabolism and catalyzes the penultimate step of the homogentisate pathway. This pathway is used for the degradation of phenylacetic acid, the side chain precursor of benzylpenicillin (see Discussion). It is also remarkable that three isoforms of a probable acetyl-CoA hydrolase Ach1 (spots Cd2, Cd3 and Cd4) are also underrepresented after induction with 1,3-DAP. This protein is involved in mitochondrial acetate detoxification by a CoASH transfer from acetyl-CoA to succinate conserving energy by the detoxification of mitochondrial acetate rather than performing the energy wasting hydrolysis of acetyl-CoA [42].

3.1.5. *Developmental processes*

1,3-DAP seems to induce the synthesis of proteins involved in the biosynthesis of the fungal cell wall and in the cytoskeletal maintenance (see Discussion). A probable glycosylphosphatidylinositol-anchored beta(1–3)glucanosyltransferase Gel3 is found 3.51-fold overrepresented (spot Dc1). Gamma-actin is only detected after 1,3-DAP addition (spot Dc15). Actin is a protein involved in crucial cellular processes such as motility, regulation of cell growth and differentiation, endocytosis, exocytosis, and structural stability [43].

3.1.6. *Effect of spermidine on the intracellular proteome of P. chrysogenum*

Since the addition of 1,3-DAP and spermidine provided a similar effect in terms of penicillin production and growth [8,9] and as shown above the spermidine synthase levels are increased after 1,3-DAP addition, proteomics studies were carried out to test the biological mechanisms induced by spermidine. Cultures of *P. chrysogenum* in the presence and absence of this polyamine were performed and the intracellular protein fractions were analyzed by 2-DE and tandem MS spectrometry. The gels obtained for both conditions were compared to each other (Fig. 4), showing 53 spots (including a total of 62 proteins) overrepresented and 35 spots (including a total of 40 proteins) underrepresented after spermidine supplementation (Fig. 5). Proteins included in those spots were grouped according to functional categories (Tables 3 and 4). Some proteins differentially represented after the addition of

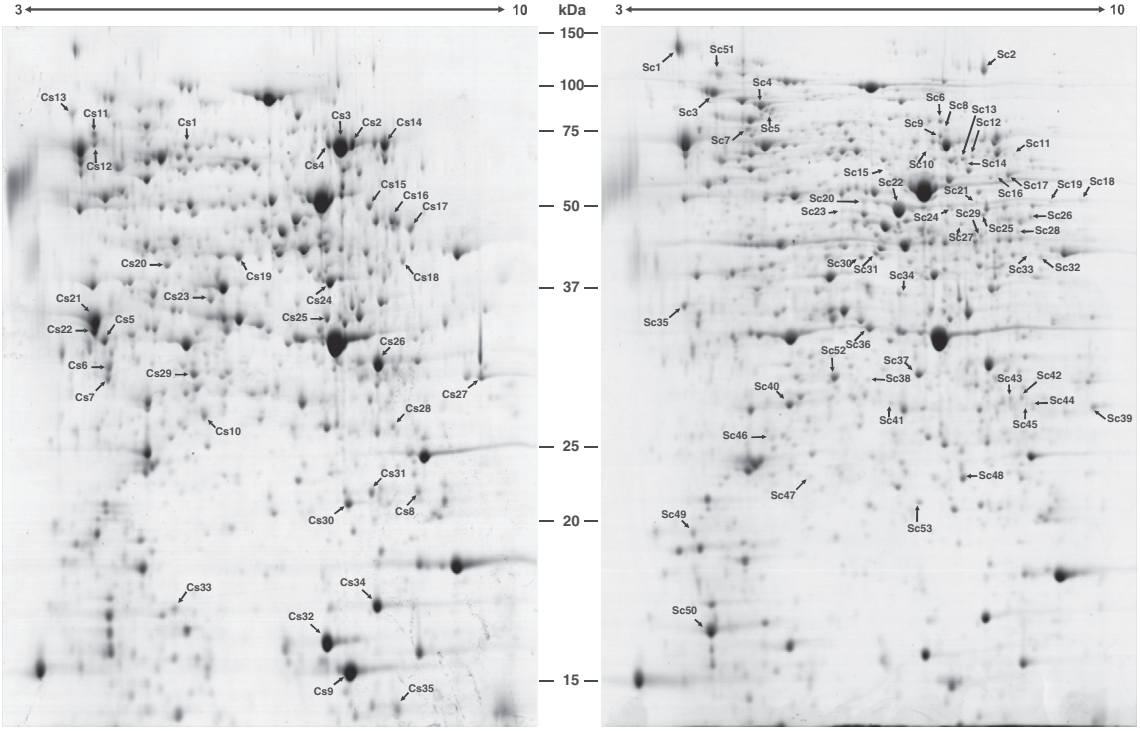

***P. chrysogenum* Wisconsin 54-1255. Intracellular proteome. Control**

***P. chrysogenum* Wisconsin 54-1255. Intracellular proteome. Spermidine**

Fig. 4 – Comparison of the intracellular proteomes of *P. chrysogenum* Wisconsin 54-1255 with or without the addition of spermidine. 2-DE gels of the intracellular proteomes of the Wisconsin 54-1255 strain grown for 40 h in the absence (control) or presence of spermidine. The designation "Cs" is used for those spots underrepresented after the addition of this polyamine, whereas "Sc" is used for those spots overrepresented after treatment with spermidine. The spots differentially represented are numbered and correspond to those proteins listed in Tables 3 and 4.

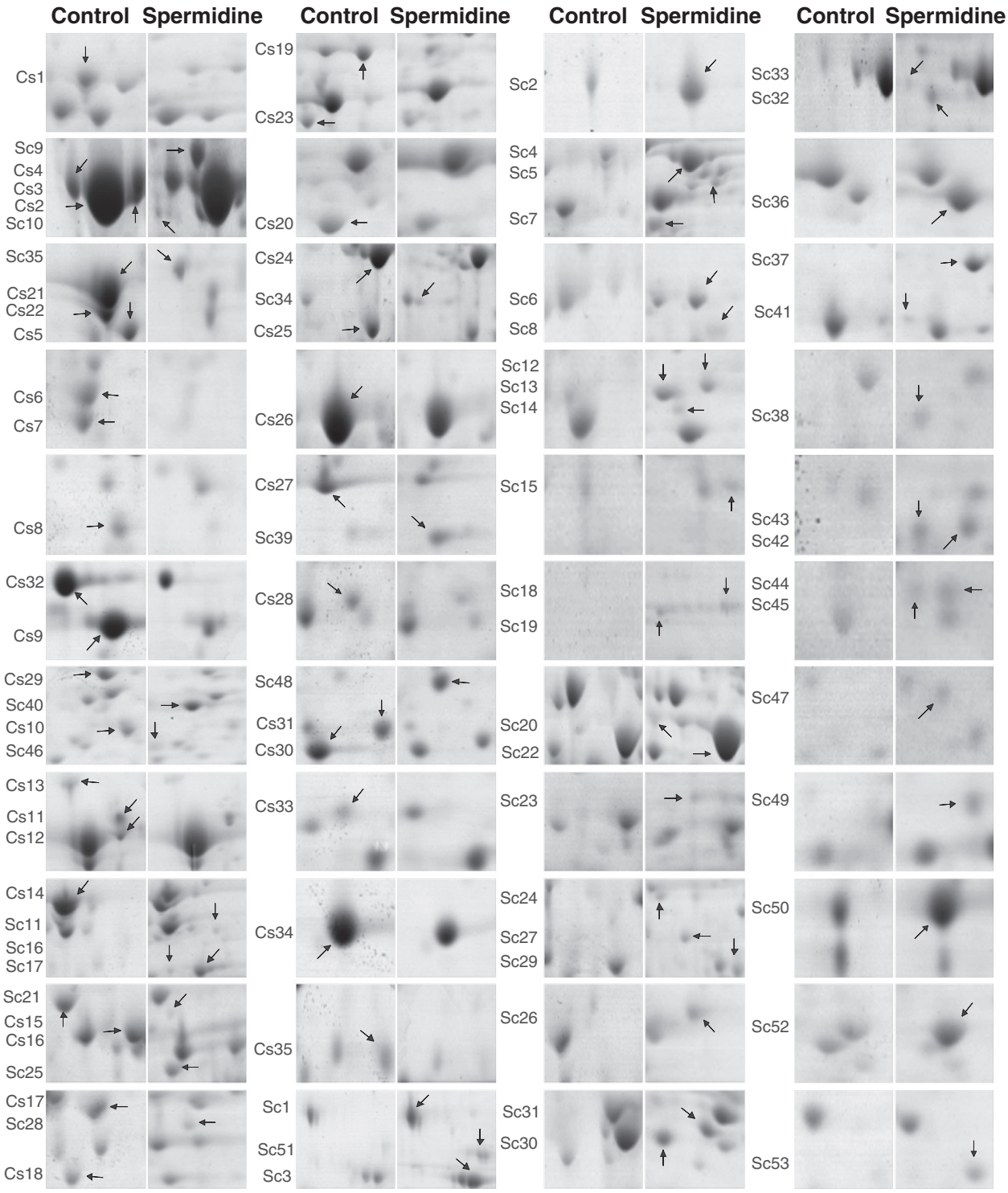

Fig. 5 – Close-up view of the spots differentially represented after addition of spermidine. Enlargement of gel portions containing the spots overrepresented in the gels of Fig. 4. The designation "Cs" is used for those spots underrepresented after the addition of this polyamine, whereas "Sc" is used for those spots overrepresented after treatment with spermidine. The spots differentially represented are numbered and correspond to those proteins listed in Tables 3 and 4.

spermidine were coincident with proteins whose synthesis was modified after 1,3-DAP supplementation and are listed in Table 5. The main findings are summarized below.

3.1.7. *Metabolism and energy*

The most relevant finding in this category is that one of the isoforms of the IAT, which is involved in the last step of

penicillin biosynthesis, is only detected after the addition of spermidine (spot Sc41). This isoform was also induced after 1,3-DAP addition (see Discussion). This result correlates well with the previously-described increase in the penicillin titers after spermidine addition [9].

Another interesting finding is that two proteins with an important role in the biosynthesis of β-lactam antibiotics are only detected after induction with spermidine. The first enzyme is a probable phosphogluconate dehydrogenase Gnd1 (spot Sc20), which catalyzes a NADPH regenerating reaction in the pentose phosphate pathway. The second protein is a probable thiamine-phosphate pyrophosphorylase/hydroxyethylthiazole kinase (spot Sc15) (see Discussion).

As it was observed for 1,3-DAP, a probable UTP-glucose-1-phosphate uridylyltransferase Ugp1 (spot Sc12) is only detected after the addition of spermidine. This enzyme, as it was indicated above, is involved in glycogenesis and it has been suggested to be essential for the completion of development of the slime mold *D. discoideum* [23–25].

The biosynthesis of acetyl-CoA seems to be favored also after the addition of spermidine. In this case, the main pathway for the production of acetyl-CoA is represented by the two isoforms of a probable ATP citrate lyase ACL1 (spots Sc28 and Sc29, only detected under supplementation with spermidine), which were also induced by 1,3-DAP, and a probable alpha subunit E1 of the pyruvate dehydrogenase complex Pda1 (spot Sc23).

The presence of three isoforms of a probable soluble cytosolic fumarate reductase, which converts fumarate to succinate, is only detected after induction with spermidine (spots Sc42, Sc43 and Sc45) and may indicate a shift in metabolism, since fumarate reductase has been reported to be important in microbial metabolism as a part of anaerobic respiration [44].

Two different alcohol dehydrogenases are only detected after the addition of spermidine. The first one is a probable alcohol dehydrogenase AlkJ (spot Sc11), which converts primary alcohols produced by the alkane utilizing system of *Pseudomonas oleovorans* (the most thoroughly characterized bacterial system for oxidation of alkanes in the C5 to C12 range) to aldehydes [45,46]. The second one is a probable ALR alcohol dehydrogenase (NADP+) (spot Sc34), which catalyzes the NADPH-dependent reduction of a variety of aromatic and aliphatic aldehydes to their corresponding alcohols. It catalyzes the reduction of mevaldate to mevalonic acid and of glyceraldehyde to glycerol and plays a role in the activation of procarcinogens, such as polycyclic aromatic hydrocarbon *trans*-dihydrodiols [47,48].

Related to β-alanine biosynthesis, two isoforms of a probable 4-aminobutyrate transaminase were 4.47-fold overrepresented (spot Sc17) or only detected (spot Sc16) after spermidine addition (see Discussion). This protein, which is required for oxidative stress tolerance and nitrogen utilization [49,50], was also found overrepresented in the presence of 1,3-DAP.

As it was observed with 1,3-DAP, purine metabolism is also favored after the addition of spermidine to the cultures. A probable guanylate kinase Guk1 (spot Sc48), which catalyzes the ATP-dependent phosphorylation of GMP into GDP and is essential for recycling GMP and indirectly, cGMP [51], is 5.74-fold overrepresented.

The finding that a probable 5-aminolevulinic acid synthase HemA is only detected after spermidine addition (spot Sc10) is interesting. This enzyme catalyses the pyridoxal phosphate-dependent condensation of succinyl-CoA and glycine to give 5-aminolevulinic acid, which is the first intermediate in the porphyrin synthesis pathway. Correlated to this result is the 2.56-fold overrepresentation of a probable coproporphyrinogen oxidase III Hem13 (spot Sc31), which is involved in the sixth step of porphyrin metabolism (see Discussion).

It is interesting that spermidine causes a 2.21-fold decrease in the levels of the cysteine synthase (spot Cs18), an enzyme forming cysteine from serine. Cysteine is formed by at least two pathways in fungi (see Discussion).

3.1.8. *Information pathways*

Some proteins involved in protein fate mechanisms that are differentially represented after the addition of spermidine are the same as those found differentially represented after the addition of 1,3-DAP (see Discussion).

As it was observed for 1,3-DAP, spermidine addition also induces the synthesis of a probable suppressor of tom1 protein Mpt4 (spots Sc39; 7.63-fold overrepresented) and Sc48 (5.74-fold overrepresented). The synthesis of a probable nascent polypeptide-associated complex alpha chain alpha-NAC (spot Sc50, 3.1-fold overrepresented), was also increased by 1,3-DAP.

Proteins specifically induced by spermidine and not by 1,3-DAP are involved in translation processes or in the regulation of protein function. The proteins specifically repressed by this polyamine are the allergen Pen n-18 (a vacuolar serine proteinase found 2.31-fold underrepresented in spot Cs26) or a probable ubiquitin conjugating enzyme Ubc4 (spot Cs33, only detected without spermidine), which mediates selective degradation of short-lived and abnormal proteins [52].

3.1.9. *Response to stimuli*

A probable glutathione reductase Glr1 is only detected after the addition of spermidine (spot Sc14), a result that is coincident with that obtained after the addition of 1,3-DAP. This protein has been found as one of the proteins overrepresented in the penicillin high-producer strain AS-P-78 [19].

Interestingly, two isoforms of a probable fumarylacetoacetase are overrepresented (spots Sc19; only detected under spermidine supplementation and Sc22; 3.35-fold overrepresented), whereas it was underrepresented after the addition of 1,3-DAP. This enzyme belongs to the homogentisate pathway catalyzing the hydrolytic cleavage of a carbon–carbon bond in fumarylacetoacetate to yield fumarate and acetoacetate as the final step in phenylacetate, phenylalanine and tyrosine degradation [41]. Related to this result is the finding of two isoforms of a 3,4-dihydroxyphenylacetate 2,3-dioxygenase HmgA (spots Sc16 and Sc30). This enzyme, also known as homogentisate dioxygenase, is only detected after the addition of spermidine and catalyzes the conversion of 2,5-dihydroxyphenylacetate into maleylacetoacetate in the homogentisate pathway. Surprisingly, another isoform of this enzyme is found 2.1-fold underrepresented by the addition of spermidine (spot Cs19). Therefore, the homogentisate pathway seems to be highly

Table 3 – Proteins overrepresented in the *P. chrysogenum* Wisconsin 54-1255 intracellular proteome after the addition of spermidine. Fold increase and p-value are indicated for those proteins detected under both conditions. Proteins that are only detected after the addition of spermidine are denoted as N/A.

Spot	ORF name	Accession no.	Title	Theoretical		Estimated								
				Mass (kDa)	pI	Mass (kDa)	pI	Peptides identified	Un-matched peptides	Score	Percent coverage (%)	Fold increase	p-value	Function
Metabolism and energy														
Sc2	Pc22g00570	gi|255946670	Strong similarity to triacylglycerol lipase lipI — *Geotrichum candidum*	61.2	6.5	10.5	7.7	22	43	1000	39	4.50	2.30E−04	Lipid metabolism
Sc6	Pc06g01600	gi|255930411	Strong similarity to FAD dependent L-sorbose dehydrogenase SDH — *Gluconobacter oxydans*	65.3	6.1	68.2	7.2	28	37	691	69	2.55	4.76E−04	L-ascorbic acid synthesis
Sc9	Pc21g01110	gi|255952859	Strong similarity to 3-methylcrotonyl-CoA carboxylase (MCC) non-biotin-containing beta subunit like protein An07g04270 — *Aspergillus niger*	62.6	7.7	62.9	7.1	22	39	813	46	N/A	N/A	Leucine metabolism
Sc10	Pc22g13500	gi|255949018	Strong similarity to 5-aminolevulinic acid synthase hemA — *Aspergillus nidulans*	69.2	8.6	59.1	7.0	23	42	436	53	N/A	N/A	Porphyrin biosynthesis
Sc11	Pc22g10020	gi|211592028	Strong similarity to alcohol dehydrogenase alkJ — *Pseudomonas oleovorans*	60.3	5.9	57.2	8.1	27	37	549	50	N/A	N/A	Alcohol metabolism
Sc12	Pc21g12790	gi|211590017	Strong similarity to UTP-glucose-1-phosphate uridylyltransferase Ugp1 — *Saccharomyces cerevisiae*	57.7	6.4	56.6	7.5	24	37	748	58	N/A	N/A	Glycogenesis
Sc15	Pc13g03600	gi|255935541	Strong similarity to thiamin-phosphate pyrophosphorylase/hydroxyethylthiazole kinase Thi6 — *Saccharomyces cerevisiae*	54.2	6.0	53.2	6.4	21	34	657	58	N/A	N/A	Thiamine biosynthesis
Sc16	Pc21g17880	gi|211590494	Strong similarity to 4-aminobutyrate trans-aminase gatA — *Aspergillus nidulans*	55.2	8.8	51.7	7.9	22	43	431	53	N/A	N/A	b-alanine biosynthesis
Sc17	Pc21g17880	gi|211590494	Strong similarity to 4-aminobutyrate trans-aminase gatA — *Aspergillus nidulans*	55.2	8.8	51.7	8.0	30	28	950	76	4.47	1.11E−04	b-alanine biosynthesis
Sc18	Pc21g17590	gi|255956007	Strong similarity to acyl-CoA dehydrogenase like protein An17g01150 — *Aspergillus niger*	49.0	8.7	47.0	8.9	25	40	889	64	N/A	N/A	Lipid metabolism
Sc20	Pc12g10940	gi|211582533	Strong similarity to phosphogluconate dehydrogenase Gnd1 — *Saccharomyces cerevisiae*	56.1	5.9	46.8	6.1	26	39	1010	58	N/A	N/A	Pentose phosphate pathway
Sc21	Pc22g16600	gi|255949614	Strong similarity to molybdopterin-converting factor activator like protein An03g03000 — *Aspergillus niger*	63.1	5.8	46.7	7.6	25	40	911	52	N/A	N/A	Cofactor biosynthesis
Sc23	Pc22g11710	gi|211592134	Strong similarity to alpha subunit E1 of the pyruvate dehydrogenase complex Pda1 — *Saccharomyces cerevisiae*	45.4	8.5	45.4	5.9	14	51	226	37	N/A	N/A	Acetyl-CoA biosynthesis
Sc25	Pc13g12930	gi|255937361	Strong similarity to peroxisomal acetyl-CoA C-acyltransferase POT1 — *Yarrowia lipolytica*	44.7	6.9	44.9	7.7	23	41	725	65	N/A	N/A	Lipid metabolism
Sc26	Pc22g06820	gi|255947884	Strong similarity to peroxisomal acetyl-CoA C-acyltransferase POT1 — *Yarrowia lipolytica*	43.5	8.1	44.6	8.3	20	44	821	52	N/A	N/A	Lipid metabolism
Sc27	Pc22g10010	gi|211592027	Strong similarity to N-acetylglucosamine-6-phosphate deacetylase CaNAG2 — *Candida albicans*	46.1	5.8	43.6	7.4	13	52	99	61	N/A	N/A	Aminosugar metabolism

Sc28	Pc21g20480	gi|255956565	Strong similarity to ATP citrate lyase ACL1 — *Sordaria macrospora*	71.9	7.6	42.5	8.1	22	41	881	36	N/A	N/A	Acetyl-CoA biosynthesis
Sc29	Pc21g20480	gi|255956565	Strong similarity to ATP citrate lyase ACL1 — *Sordaria macrospora*	71.9	7.6	42.0	7.6	8	26	143	15	N/A	N/A	Acetyl-CoA biosynthesis
Sc31	Pc12g05380	gi|211582002	Strong similarity to coproporphyrinogen oxidase III Hem13 — *Saccharomyces cerevisiae*	50.0	7.2	39.5	6.4	10	45	218	25	2.56	2.96E−05	Porphyrin biosynthesis
Sc33	Pc13g05940	gi|255936003	Strong similarity to trifunctional protein of the beta-oxidation *fox-2* — *Neurospora crassa*	97.3	8.6	39.8	8.3	10	41	155	14	N/A	N/A	Lipid metabolism
Sc34	Pc21g01220	gi|211588904	Strong similarity to alcohol dehydrogenase (NADP+) ALR — *Sus scrofa*	35.4	6.0	35.3	6.7	8	57	194	38	N/A	N/A	Alcohol metabolism
Sc40	Pc12g00830	gi|211581603	Strong similarity to sorbitol utilization protein *sou2* — *Candida albicans*	28.7	5.3	27.4	5.2	20	39	820	83	3.15	1.04E−03	Carbohydrate metabolism
Sc41	Pc13g08270	gi|211583872	Adenylylsulfate kinase AAA81521 — *Penicillium chrysogenum*	23.6	6.0	26.8	6.5	12	53	365	56	N/A	N/A	Purine, seleno amino acids and sulfur metabolism
	Pc21g21370	gi|211590823	Acyl-coenzyme A:isopenicillin N acyltransferase (acyltransferase) AAT/PenDE — *Penicillium chrysogenum*	40.2	6.2	26.8	6.5	9	56	78	33	N/A	N/A	Penicillin biosynthesis
Sc42	Pc12g03090	gi|211581814	Strong similarity to soluble cytoplasmic fumarate reductase YEL047c — *Saccharomyces cerevisiae*	66.8	6.2	27.1	8.2	14	22	519	20	N/A	N/A	Anaerobic respiration
Sc43	Pc12g03090	gi|211581814	Strong similarity to soluble cytoplasmic fumarate reductase YEL047c — *Saccharomyces cerevisiae*	66.8	6.2	27.0	8.0	11	19	385	18	N/A	N/A	Anaerobic respiration
Sc44	Pc12g05310	gi|255931643	Strong similarity to adenylate kinase Adk1 — *Saccharomyces cerevisiae*	28.6	7.0	26.8	8.3	14	42	538	54	N/A	N/A	Purine metabolism
Sc45	Pc12g03090	gi|211581814	Strong similarity to soluble cytoplasmic fumarate reductase YEL047c — *Saccharomyces cerevisiae*	66.8	6.2	26.8	8.2	13	37	350	18	N/A	N/A	Anaerobic respiration
Sc46	Pc21g03400	gi|211589115	Strong similarity to triose-phosphate-isomerase *tpiA* from patent WO8704464-A — *Aspergillus niger*	27.2	5.3	24.4	5.0	11	46	154	50	N/A	N/A	Carbohydrate metabolism
Sc48	Pc16g01840	gi|211585181	Strong similarity to guanylate kinase Guk1 — *Saccharomyces cerevisiae*	22.0	6.2	22.2	7.5	6	59	191	42	5.74	2.55E−05	Purine metabolism
Sc51	Pc18g02580	gi|211586833	Strong similarity to acid phosphatase AFPhoA — *Aspergillus ficuum*	50.2	5.0	98.3	4.2	6	20	260	13	N/A	N/A	Phosphate metabolism
Information pathways														
Sc4	Pc22g19990	gi|211592918	Strong similarity to endonuclease SceI 75 kDa subunit Ens1 — *Saccharomyces cerevisiae*	72.6	5.6	73.3	4.8	26	36	725	47	N/A	N/A	Protein fate
Sc5	Pc22g10220	gi|211592047	Strong similarity to dnaK-type molecular chaperone Ssb2 — *Saccharomyces cerevisiae*	67.0	5.3	72.4	5.0	27	36	1090	57	N/A	N/A	Protein fate
Sc7	Pc22g10220	gi|211592047	Strong similarity to dnaK-type molecular chaperone Ssb2 — *Saccharomyces cerevisiae*	67.0	5.3	64.1	4.7	18	13	991	44	4.51	5.71E−03	Protein fate
Sc13	Pc21g02360	gi|211589011	Strong similarity to GU4 nucleic-binding protein 1 Arc1 — *Saccharomyces cerevisiae*	47.8	6.4	55.9	7.4	25	39	952	77	N/A	N/A	Protein with binding function or cofactor requirement

(continued on next page)

Table 3 (*continued*)

Spot	ORF name	Accession no.	Title	Theoretical		Estimated								
				Mass (kDa)	pI	Mass (kDa)	pI	Peptides identified	Un-matched peptides	Score	Percent coverage (%)	Fold increase	p-value	Function
Information pathways														
Sc19	Pc21g19210	gi|211590623	Strong similarity to 442K curved DNA-binding protein SPAC23H4.09 — *Schizosaccharomyces pombe*	44.2	8.3	46.8	8.5	13	40	375	46	N/A	N/A	Protein with binding function or cofactor requirement
Sc30	Pc12g05300	gi|211581996	Strong similarity to 26S proteasome regulatory chain 12 rpn12 — *Homo sapiens*	39.2	5.5	40.7	5.8	16	27	568	56	N/A	N/A	Regulation of metabolism and protein function
Sc32	Pc21g11890	gi|255954935	Strong similarity to RNA binding protein 47 RBP47 — *Nicotiana plumbaginifolia*	44.0	6.0	39.3	8.4	11	35	220	30	N/A	N/A	Protein with binding function or cofactor requirement
Sc34	Pc13g10770	gi|211584117	Strong similarity to cAMP-dependent protein kinase regulatory subunit pkaR — *Aspergillus niger*	44.5	5.0	35.3	6.7	11	54	161	30	N/A	N/A	Regulation of metabolism and protein function
Sc35	Pc13g08810	gi|211583926	Strong similarity to elongation factor 1beta EF-1 — *Oryctolagus cuniculus*	25.0	4.4	34.2	3.8	8	45	843	59	N/A	N/A	Protein synthesis
Sc36	Pc12g12040	gi|211582639	Strong similarity to translation elongation factor eEF-2 — *Cricetulus griseus*	94.4	6.3	32.2	6.3	21	44	842	25	2.80	1.10E−04	Protein synthesis
Sc39	Pc18g00860	gi|255942327	Weak similarity to suppressor of tom1 protein Mpt4 — *Saccharomyces cerevisiae*	34.5	9.7	27.1	9.3	8	25	153	21	7.63	7.00E−04	Protein synthesis
Sc48	Pc18g00860	gi|255942327	Weak similarity to suppressor of tom1 protein Mpt4 — *Saccharomyces cerevisiae*	34.5	9.7	22.2	7.5	10	55	389	28	5.74	2.55E−05	Protein synthesis
Sc49	Pc21g03140	gi|211589089	Strong similarity to cell cycle regulator p21 protein wos2p — *Schizosaccharomyces pombe*	22.0	4.5	17.9	4.0	8	51	163	39	N/A	N/A	Cell cycle and DNA processing
Sc50	Pc20g13270	gi|211588542	Strong similarity to nascent polypeptide-associated complex alpha chain alpha-NAC — *Mus musculus*	22.0	4.7	13.3	4.2	3	51	93	20	3.11	4.53E−05	Transcription
Perception and response to stimuli														
Sc1	Pc18g02900	gi|211586864	Lysophospholipase phospholipase B plb1 — *Penicillium chrysogenum*	68.7	4.4	12.2	3.8	7	27	610	14	3.07	1.41E−03	Cell rescue, defence and virulence
Sc8	Pc12g03130	gi|211581818	Strong similarity to acetyl-CoA hydrolase Ach1 — *Saccharomyces cerevisiae*	58.3	6.2	65.0	7.2	19	22	530	38	N/A	N/A	Cell rescue, defence and virulence

Sc14	Pc16g13280	gi|211586250	Strong similarity to glutathione reductase Glr1 — *Saccharomyces cerevisiae*	51.5	6.2	54.6	7.5	22	40	939	63	N/A	N/A	Cell rescue, defence and virulence
Sc16	Pc12g09040	gi|255932351	Strong similarity to 3,4-dihydroxyphenylacetate 2,3-dioxygenase hmgA — *Aspergillus nidulans*	50.4	5.9	51.7	7.9	9	56	203	28	N/A	N/A	Homogentisate pathway
Sc19	Pc12g09030	gi|211582350	Strong similarity to fumarylacetoacetase — *Homo sapiens*	46.6	6.0	46.8	8.5	9	47	121	37	N/A	N/A	Homogentisate pathway
Sc22	Pc12g09030	gi|211582350	Strong similarity to fumarylacetoacetase — *Homo sapiens*	46.6	6.0	44.5	6.7	14	17	812	50	3.35	1.88E−04	Homogentisate pathway
Sc27	Pc13g12030	gi|211584240	Strong similarity to flavohemoglobin Fhp — *Alcaligenes eutrophus*	47.8	7.8	43.6	7.4	18	45	686	53	N/A	N/A	Cell rescue, defence and virulence
Sc30	Pc12g09040	gi|255932351	Strong similarity to 3,4-dihydroxyphenylacetate 2,3-dioxygenase hmgA — *Aspergillus nidulans*	50.4	5.9	40.7	5.8	7	44	168	22	N/A	N/A	Homogentisate pathway
Developmental processes															
Sc3	Pc22g09380	gi|211591967	Strong similarity to glycosylphosphatidylinositol-anchored beta(1–3)glucanosyltransferase gel3 — *Aspergillus fumigatus*	57.6	4.9	79.9	4.3	10	30	427	21	3.45	2.14E−05	Biogenesis of cellular components
Other proteins															
Sc24	Pc14g02010	gi|211584816	Strong similarity to hypothetical protein contig_1_98_scaffold_6.tfa_1090cg — *Aspergillus nidulans*	44.2	6.2	45.7	7.3	15	50	466	60	N/A	N/A	Unknown
Sc37	Pc12g08070	gi|211582258	Weak similarity to hypothetical protein Ta1372 — *Thermoplasma acidophilum*	27.3	5.0	28.7	6.8	13	51	771	61	N/A	N/A	Unknown
Sc38	Pc21g02210	gi|211588997	Strong similarity to hypothetical protein contig31_part_ii.tfa_2190wg — *Aspergillus fumigatus*	34.7	5.6	28.4	6.2	8	52	375	39	N/A	N/A	Unknown
Sc47	Pc22g03110	gi|211591371	Strong similarity to hypothetical protein An01g08830 — *Aspergillus niger*	24.3	7.9	21.5	5.5	9	44	282	43	N/A	N/A	Unknown
Sc50		gi|144952798	16 kDa allergen — *Penicillium chrysogenum*	16.4	5.2	13.3	4.2	4	48	395	21	3.11	4.53E−05	Unknown
Sc52	Pc21g12310	gi|255955019	Hypothetical protein *Penicillium chrysogenum*	30.4	5.6	29.0	5.8	20	43	831	69	3.02	2.54E−04	Unknown
Sc53	Pc23g00350	gi|255951667	Hypothetical protein BAC82546 — *Penicillium chrysogenum*	22.5	6.1	19.8	6.9	10	28	549	45	N/A	N/A	Unknown
	Pc24g02750	gi|34392437	Hypothetical protein [*Penicillium chrysogenum*]	23.2	5.6	19.8	6.9	8	32	369	34	N/A	N/A	Unknown

Table 4 – Proteins underrepresented in the *P. chrysogenum* Wisconsin 54-1255 intracellular proteome after the addition of spermidine. Fold decrease and p-value are indicated for those proteins detected under both conditions. Proteins that are not detected after the addition of spermidine are denoted as N/A.

Spot	ORF name	Accession no.	Title	Theoretical		Estimated								
				Mass (kDa)	pI	Mass (kDa)	pI	Peptides identified	Un-matched peptides	Score	Percent coverage (%)	Fold decrease	p-value	Function
Metabolism and energy														
Cs1	Pc22g02000	gi|211591261	Strong similarity to mitochondrial aconitate hydratase Aco1 — *Saccharomyces cerevisiae*	85.9	6.0	61.4	5.2	26	34	912	35	3.65	6.64E−05	Krebs cycle
Cs10	Pc16g12780	gi|255941616	Strong similarity to core protein I of ubiquinol-cytochrome-c reductase beta-MPP — *Neurospora crassa*	53.1	5.7	25.8	5.5	10	44	443	25	2.42	4.06E−04	Oxidative phosphorylation
Cs13	Pc21g13670	gi|255955263	Strong similarity to enzyme with sugar transferase activity like protein An01g10930 — *Aspergillus niger*	107.3	4.9	72.4	3.7	15	50	473	15	2.47	9.37E−03	Carbohydrate metabolism
Cs14	Pc22g03660	gi|211591424	Strong similarity to isocitrate lyase *acuD* — *Aspergillus nidulans*	60.1	6.5	61.4	7.8	24	40	727	62	2.23	1.41E−04	Glyoxylate and dicarboxilate metabolism
Cs15	Pc16g07470	gi|211585695	Strong similarity to glycine decarboxylase subunit T Gcv1 — *Saccharomyces cerevisiae*	51.6	8.9	46.7	7.6	23	42	885	71	2.21	1.17E−04	Glycine to 5,10 methylene tetrahydrofolate catabolism
Cs16	Pc20g13510	gi|211588565	Strong similarity to methylcitrate synthase *mcsA* — *Aspergillus nidulans*	51.0	8.4	44.5	7.9	23	39	492	55	3.25	1.18E−05	Propionate to pyruvate oxidation through methylcitrate cycle
Cs17	Pc22g06820	gi|255947884	Strong similarity to peroxisomal acetyl-CoA C-acyltransferase POT1 — *Yarrowia lipolytica*	43.5	8.1	43.6	8.2	13	52	519	45	2.12	1.21E−03	Lipid metabolism
	Pc16g05560	gi|211585518	Strong similarity to mitochondrial sulfide dehydrogenase (coenzyme Q2) SPBC2G5.06c — *Schizosaccharomyces pombe*	48.3	8.8	43.6	8.2	22	43	389	53	2.12	1.21E−03	Oxidative phosphorylation
Cs18	Pc21g14890	gi|211590213	Cysteine synthase BAC82550 — *Penicillium chrysogenum*	40.1	8.6	39.1	8.1	22	16	1100	73	2.21	5.76E−05	Cysteine biosynthesis
Cs20	Pc21g17460	gi|211590454	Strong similarity to adenosine kinase like protein An17g01330 — *Aspergillus niger*	38.4	5.4	38.6	5.0	16	49	661	53	2.05	2.82E−04	Purine metabolism
Cs23	Pc22g04850	gi|211591539	Strong similarity to D-arabinose dehydrogenase Ara1 — *Saccharomyces cerevisiae*	36.6	5.5	35.0	5.6	16	49	716	48	2.07	5.00E−03	Carbohydrate metabolism
Cs28	Pc22g02000	gi|211591261	Strong similarity to mitochondrial aconitate hydratase Aco1 — *Saccharomyces cerevisiae*	85.9	6.0	25.1	7.9	13	44	254	18	2.07	8.15E−04	Krebs cycle
Cs29	Pc18g01220	gi|211586700	Strong similarity to fructose-bisphosphate aldolase Fba1 — *Saccharomyces cerevisiae*	39.5	5.4	28.8	5.3	9	40	203	28	2.09	1.21E−04	Glycolysis and gluconeogenesis
Information pathways														
Cs5	Pc22g19990	gi|211592918	Strong similarity to endonuclease SceI 75 kDa subunit Ens1 — *Saccharomyces cerevisiae*	72.6	5.6	31.4	4.2	14	51	425	21	6.34	4.39E−05	Protein fate
Cs6	Pc22g11240	gi|211592088	Strong similarity to heat shock protein 70 *hsp70* — *Ajellomyces capsulatus* (allergen Pen c 19)	69.7	5.0	29.3	4.2	14	43	480	29	5.88	4.34E−03	Protein fate

Cs7	Pc22g11240	gi|211592088	Strong similarity to heat shock protein 70 *hsp70* — *Ajellomyces capsulatus* (allergen Pen c 19)	69.7	5.0	28.4	4.2	17	48	557	35	4.57	1.86E−04	Protein fate
Cs8	Pc21g11890	gi|255954935	Strong similarity to RNA binding protein 47 RBP47 — *Nicotiana plumbaginifolia*	44.0	6.0	20.2	8.3	11	53	415	27	4.83	7.44E−07	Protein with binding function or cofactor requirement
Cs11	Pc22g02800	gi|211591341	Calreticulin [*Penicillium chrysogenum*]. strong similarity to calcium-binding protein precursor cnx1p — *Schizosaccharomyces pombe*	62.0	4.8	65.6	4.0	10	47	349	20	2.68	1.33E−03	Protein fate
	Pc21g11280	gi|211589871	Strong similarity to protein disulfide isomerase A pdiA — *Aspergillus niger*	56.6	4.7	65.6	4.0	11	46	272	27	2.68	1.33E−03	Protein fate
Cs12	Pc21g11280	gi|211589871	Strong similarity to protein disulfide isomerase A pdiA — *Aspergillus niger*	56.6	4.7	61.8	4.0	20	45	507	48	2.29	8.56E−03	Protein fate
Cs21	Pc22g11240	gi|211592088	Strong similarity to heat shock protein 70 *hsp70* — *Ajellomyces capsulatus* (allergen Pen c 19)	69.7	5.0	32.9	4.1	13	24	384	31	9.68	1.58E−04	Protein fate
Cs22	Pc22g11240	gi|211592088	Strong similarity to heat shock protein 70 *hsp70* — *Ajellomyces capsulatus* (allergen Pen c 19)	69.7	5.0	32.1	4.0	18	47	565	40	2.41	5.54E−03	Protein fate
Cs26	Pc21g16970	gi|7963902	Vacuolar serine proteinase AAG44693 — *Penicillium chrysogenum*. Allergen Pen n 18	52.5	6.1	29.4	7.7	8	36	221	23	2.31	1.44E−05	Protein fate
Cs33	Pc18g01180	gi|211586697	Strong similarity to ubiquitin conjugating enzyme Ubc4 — *Saccharomyces cerevisiae*	17.4	5.3	13.7	5.1	5	47	90	46	N/A	N/A	Protein fate
Cs34	Pc16g13060	gi|211586228	Strong similarity to cyclophilin cypB — *Aspergillus nidulans*	18.1	6.9	13.7	7.7	10	55	352	51	2.29	9.72E−05	Protein fate
Perception and response to stimuli															
Cs2	Pc12g03130	gi|211581818	Strong similarity to acetyl-CoA hydrolase Ach1 — *Saccharomyces cerevisiae*	58.3	6.2	61.8	7.4	26	39	805	72	5.06	9.04E−05	Cell rescue, defense and virulence
Cs3	Pc12g03130	gi|211581818	Strong similarity to acetyl-CoA hydrolase Ach1 — *Saccharomyces cerevisiae*	58.3	6.2	60.4	7.3	30	32	822	80	3.23	4.23E−06	Cell rescue, defense and virulence
Cs4	Pc12g03130	gi|211581818	Strong similarity to acetyl-CoA hydrolase Ach1 — *Saccharomyces cerevisiae*	58.3	6.2	61.8	7.1	30	33	816	80	4.23	1.34E−03	Cell rescue, defense and virulence
Cs19	Pc12g09040	gi|255932351	Strong similarity to 3,4-dihydroxyphenylacetate 2,3-dioxygenase hmgA — *Aspergillus nidulans*	50.4	5.9	39.6	5.9	18	47	671	58	2.10	3.52E−04	Homogentisate pathway
Cs24	Pc20g15580	gi|211588765	Strong similarity to NADPH-dependent aldehyde reductase — *Sporobolomyces salmonicolor*	37.3	6.1	36.5	7.1	19	46	1020	72	2.18	3.25E−05	Cell rescue, defense and virulence
Cs31	Pc22g04680	gi|211591523	Strong similarity to superoxide dismutase like protein An04g04870 — *Aspergillus niger*	24.7	8.7	20.2	7.7	4	36	148	27	2.15	8.01E−07	Cell rescue, defense and virulence
Cs32	Pc21g16940	gi|255955883	Strong similarity to Cu,Zn superoxide dismutase *sodC* — *Aspergillus fumigatus*	16.0	5.9	12.1	7.1	10	55	454	87	2.48	9.42E−04	Cell rescue, defense and virulence
Developmental processes															
Cs33	Pc22g00190	gi|255946596	Strong similarity to hypothetical cell wall protein binB — *Aspergillus nidulans*	19.1	5.6	13.7	5.1	3	48	152	12	N/A	N/A	Biogenesis of cellular components

(continued on next page)

Table 4 (*continued*)

Spot	ORF name	Accession no.	Title	Theoretical		Estimated								
				Mass (kDa)	pI	Mass (kDa)	pI	Peptides identified	Un-matched peptides	Score	Percent coverage (%)	Fold decrease	p-value	Function
Other proteins														
Cs9	Pc12g00650	gi|211581586	Similarity to hypothetical protein CC3092 — *Caulobacter crescentus*	15.0	6.1	11.0	7.4	7	22	617	67	4.21	8.48E−05	Unknown
Cs12	Pc22g17870	gi|211592713	Strong similarity to hypothetical ECM33 homolog SPCC1223.12c — *Schizosaccharomyces pombe*	41.2	4.6	61.8	4.0	13	52	297	39	2.29	8.56E−03	Unknown
Cs25	Pc22g17250	gi|255949742	Strong similarity to hypothetical protein mg02084.1 — *Magnaporthe grisea*	35.9	6.5	33.3	7.1	11	45	489	45	2.08	2.16E−04	Unknown
Cs27	Pc22g17950	gi|211592721	Strong similarity to hypothetical protein contig40.tfa_680wg — *Aspergillus fumigatus*	36.0	9.5	28.5	9.1	8	29	299	30	2.34	5.44E−03	Unknown
Cs30	Pc23g00350	gi|255951667	Hypothetical protein BAC82546 — *Penicillium chrysogenum*	22.5	6.1	19.4	7.4	13	52	571	49	2.14	7.64E−04	Unknown
	Pc24g02750	gi|34392437	Hypothetical protein [*Penicillium chrysogenum*]	23.2	5.6	19.4	7.4	11	54	540	37	2.14	7.64E−04	Unknown
Cs35	Pc23g00350	gi|255951667	Hypothetical protein BAC82546 — *Penicillium chrysogenum*	22.5	6.1	9.8	8.0	9	56	375	32	3.25	8.38E−04	Unknown

Table 5 – Common proteins differentially represented after the addition of either 1,3-DAP or spermidine. Proteins have been ordered according to the ORF number.

ORF name	Accession no.	Title
Pc06g01600	gi|255930411	Strong similarity to FAD dependent L-sorbose dehydrogenase SDH — *Gluconobacter oxydans*
Pc12g00650	gi|211581586	Similarity to hypothetical protein CC3092 — *Caulobacter crescentus*
Pc12g00830	gi|211581603	Strong similarity to sorbitol utilization protein *sou2* — *Candida albicans*
Pc12g03130	gi|211581818	Strong similarity to acetyl-CoA hydrolase Ach1 — *Saccharomyces cerevisiae*
Pc12g08070	gi|211582258	Weak similarity to hypothetical protein Ta1372 — *Thermoplasma acidophilum*
Pc12g09030	gi|211582350	Strong similarity to fumarylacetoacetase — *Homo sapiens*
Pc12g09040	gi|255932351	Strong similarity to 3,4-dihydroxyphenylacetate 2,3-dioxygenase hmgA — *Aspergillus nidulans*
Pc13g08270	gi|211583872	Adenylylsulfate kinase AAA81521 — *Penicillium chrysogenum*
Pc13g08810	gi|211583926	Strong similarity to elongation factor 1beta EF-1 — *Oryctolagus cuniculus*
Pc16g07470	gi|211585695	Strong similarity to glycine decarboxylase subunit T Gcv1 — *Saccharomyces cerevisiae*
Pc16g13060	gi|211586228	Strong similarity to cyclophilin cypB — *Aspergillus nidulans*
Pc16g13280	gi|211586250	Strong similarity to glutathione reductase Glr1 — *Saccharomyces cerevisiae*
Pc18g00860	gi|255942327	Weak similarity to suppressor of tom1 protein Mpt4 — *Saccharomyces cerevisiae*
Pc20g13270	gi|211588542	Strong similarity to nascent polypeptide-associated complex alpha chain alpha-NAC — *Mus musculus*
Pc20g13510	gi|211588565	Strong similarity to methylcitrate synthase *mcsA* — *Aspergillus nidulans*
Pc21g01110	gi|255952859	Strong similarity to 3-methylcrotonyl-CoA carboxylase (MCC) non-biotin-containing beta subunit like protein An07g04270 — *Aspergillus niger*
Pc21g02210	gi|211588997	Strong similarity to hypothetical protein contig31_part_ii.tfa_2190wg — *Aspergillus fumigatus*
Pc21g02360	gi|211589011	Strong similarity to GU4 nucleic-binding protein 1 Arc1 — *Saccharomyces cerevisiae*
Pc21g03140	gi|211589089	Strong similarity to cell cycle regulator p21 protein wos2p — *Schizosaccharomyces pombe*
Pc21g11280	gi|211589871	Strong similarity to protein disulfide isomerase A pdiA — *Aspergillus niger*
Pc21g11890	gi|255954935	Strong similarity to RNA binding protein 47 RBP47 — *Nicotiana plumbaginifolia*
Pc21g12310	gi|255955019	Hypothetical protein *Penicillium chrysogenum*
Pc21g12790	gi|211590017	Strong similarity to UTP-glucose-1-phosphate uridylyltransferase Ugp1 — *Saccharomyces cerevisiae*
Pc21g17880	gi|211590494	Strong similarity to 4-aminobutyrate transaminase gatA — *Aspergillus nidulans*
Pc21g20480	gi|255956565	Strong similarity to ATP citrate lyase ACL1 — *Sordaria macrospora*
Pc21g21370	gi|211590823	Acyl-coenzyme A:isopenicillin N acyltransferase (acyltransferase) AAT/PenDE — *Penicillium chrysogenum*
Pc22g02800	gi|211591341	Calreticulin [*Penicillium chrysogenum*]. strong similarity to calcium-binding protein precursor cnx1p — *Schizosaccharomyces pombe*
Pc22g03660	gi|211591424	Strong similarity to isocitrate lyase *acuD* — *Aspergillus nidulans*
Pc22g06820	gi|255947884	Strong similarity to peroxisomal acetyl-CoA C-acyltransferase POT1 — *Yarrowia lipolytica*
Pc22g09380	gi|211591967	Strong similarity to glycosylphosphatidylinositol-anchored beta(1–3)glucanosyltransferase gel3 — *Aspergillus fumigatus*
Pc22g10220	gi|211592047	Strong similarity to dnaK-type molecular chaperone Ssb2 — *Saccharomyces cerevisiae*
Pc22g11240	gi|211592088	Strong similarity to heat shock protein 70 *hsp70* — *Ajellomyces capsulatus* (allergen Pen c 19)
Pc22g19990	gi|211592918	Strong similarity to endonuclease SceI 75 kDa subunit Ens1 — *Saccharomyces cerevisiae*
Pc23g00350	gi|255951667	Hypothetical protein BAC82546 — *Penicillium chrysogenum*
Pc24g02750	gi|34392437	Hypothetical protein [*Penicillium chrysogenum*]
	gi|144952798	16 kDa allergen — *Penicillium chrysogenum*

modified by spermidine by changing the normal form of this protein to another isoform. As indicated before, this pathway is used for the degradation of phenylacetic acid, the side chain precursor of benzylpenicillin (see Discussion).

Other proteins underrepresented after the induction with spermidine are three isoforms of a probable acetyl-CoA hydrolase Ach1 (spots Cs2, Cs3 and Cs4). This result was also found with 1,3-DAP and as indicated before, this protein is involved in mitochondrial acetate detoxification by a CoASH transfer from acetyl-CoA to succinate, conserving energy by the detoxification of mitochondrial acetate rather than performing the energy wasting hydrolysis of acetyl-CoA [42].

3.1.10. *Developmental processes*

As it was observed with 1,3-DAP, spermidine seems to induce the synthesis of proteins involved in the biosynthesis of theungal cell wall. A probable glycosylphosphatidylinositol-anchored beta(1–3)glucanosyltransferase Gel3, was found 3.45-fold overrepresented after spermidine supplementation (spot Sc3) (see Discussion). On the contrary, a hypothetical cell wall protein BinB is underrepresented after the addition of spermidine. This protein shows 74% similarity and 62% identity with the PhiA protein from *A. nidulans*, which has been reported to be essential for phialide development in this fungus [53].

3.1.11. *Morphology and sporulation are affected by 1,3-DAP and spermidine*

An interesting phenomenon that was observed after the addition of either 1,3-DAP or spermidine was the formation of large vesicles inside hyphae (Fig. 6A). Unlike control cultures, vesicles in 1,3-DAP or spermidine-supplemented cells were already observed at early time points (24 h) and were especially abundant after 48 h of growth. At 72 h, vesicles were also observed in control cultures. The presence of large vesicles

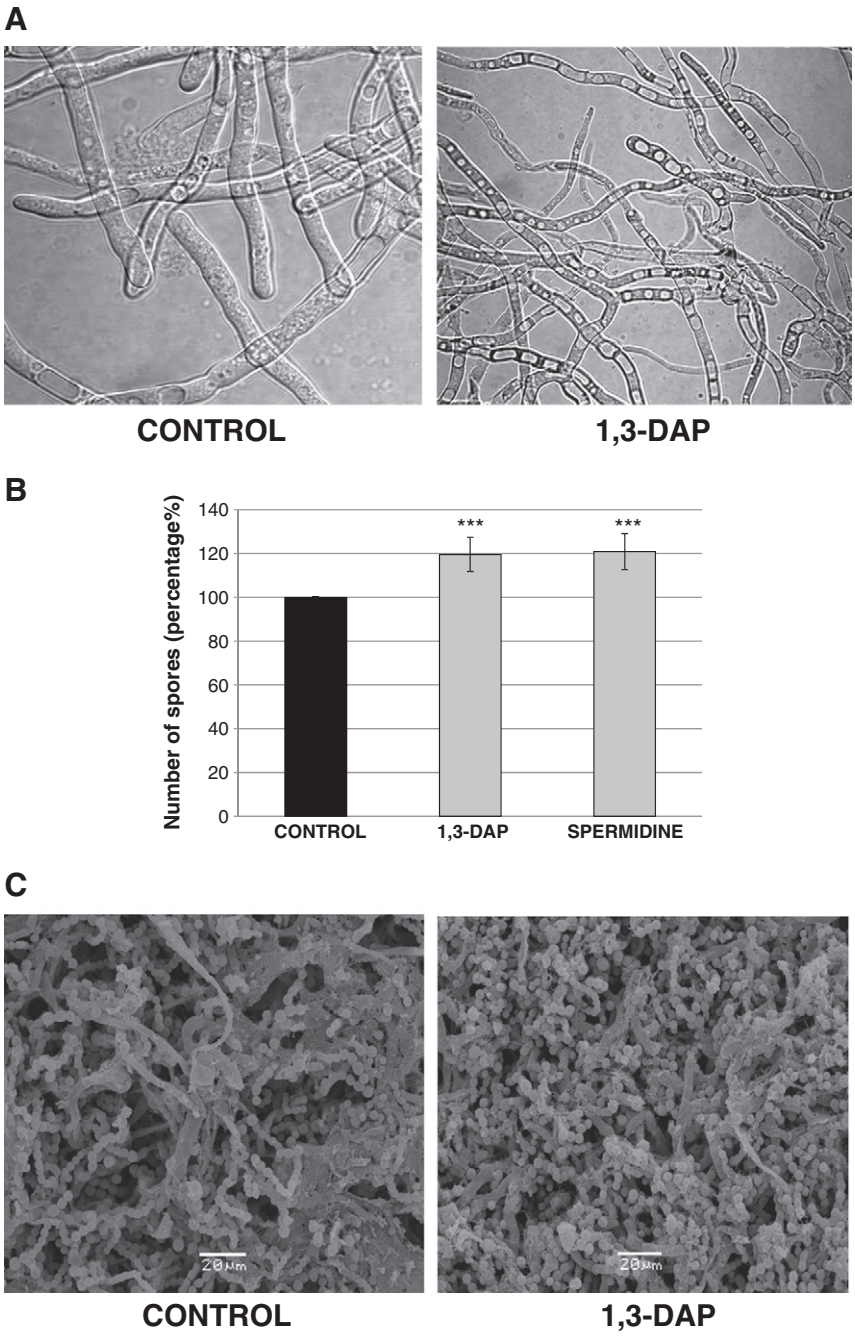

Fig. 6 – Modifications in morphology and sporulation induced by 1,3-DAP and spermidine. A) Confocal optical microscopy pictures of the *P. chrysogenum* mycelium grown in submerged cultures for 48 h without (control) or with 1,3-DAP. Spermidine gave rise to similar morphological modifications to 1,3-DAP (not shown). B) Sporulation level of *P. chrysogenum* Wisconsin 54-1255 after six days in the presence of either 1,3-DAP or spermidine. C) Scanning electron microscopy pictures of Petri dishes sown with 1×10^8 spores of *P. chrysogenum* Wisconsin 54-1255 after six days of growth without (control) or with 1,3-DAP. Spermidine gave rise to similar morphological modifications to 1,3-DAP (not shown).

inside hyphae may be related to an increase in the secretion processes of several compounds, including penicillin (see Discussion).

Another process also influenced by 1,3-DAP and spermidine was sporulation. The number of spores that were collected after six days of growth at 25 °C from Petri dishes showed a significant increase (19%, $p < 0.05$) when 5 mM 1,3-DAP or spermidine were added to the solid medium (Fig. 6B and C). This phenomenon may be related to our previous finding showing a positive effect of 1,3-DAP on the expression of the *laeA* gene [8], which controls secondary metabolism and sporulation [10]. Indeed the 1,3-DAP-mediated induction of

sporulation was not observed in the *P. chrysogenum laeA*-gene defective mutant (data not shown).

4. Discussion

It is well known that numerous metabolic processes are controlled by polyamines, such as the stabilization of macromolecules under stress conditions, the stabilization of the cellular membrane or the stabilization of nucleic acids; the latter affects gene expression, recombination and DNA repair mechanisms [54–59]. In this work, we have deciphered some modifications induced by the penicillin inducers 1,3-DAP and spermidine in *P. chrysogenum* [9] using a proteomics approach, paying special attention to those mechanisms related to the biosynthesis of penicillin. This proteomics approach has been based on 2-DE, which covers around the 10% of the potential proteins coded in the *P. chrysogenum* genome as we reported in a previous work [19].

Since 1,3-DAP induces the synthesis of the spermidine synthase, it is likely that the biosynthesis of spermidine is also increased following 1,3-DAP addition. In fact, it has been reported that N-(n-butyl)-1,3-DAP increases the spermidine levels and inhibits the synthesis of spermine [60]. 1,3-DAP is a by-product generated after the oxidation of spermidine by means of the polyamino-oxidase [61] and according to our results, it exerts a positive regulatory role on the spermidine synthase. This may suggest that many of the modifications observed after the addition of 1,3-DAP could be really attributed to an increase in the spermidine levels. In fact, several proteins differentially represented after the induction with spermidine were coincident with proteins whose synthesis was modified after 1,3-DAP addition (Table 5), thus supporting this suggestion. Other proteins, however, showed a specific pattern of expression after induction with each of the two inducers that may be attributed to specific response mechanisms of either 1,3-DAP or spermidine.

Focusing on the common effects of these two polyamines, there are common mechanisms that may explain their beneficial effect on penicillin biosynthesis. The first mechanism is directly affecting one of the penicillin biosynthetic enzymes, the IAT. This enzyme is synthesized as a 40-kDa precursor (proacyltransferase, proIAT) which undergoes an autocatalytic self-processing between residues Gly102-Cys103 in *P. chrysogenum*. The processed protein forms a heterodimer with subunits α (11 kDa, corresponding to the N-terminal fragment) and β (29 kDa, corresponding to the C-terminal region) [62–65]. A deep analysis of the 2-DE gels revealed that one new isoform of the β-subunit of IAT (only this subunit is detected in 2-DE gels [19]) appears after the addition of either 1,3-DAP or spermidine (Fig. 7), whereas the main isoform remains largely unchanged (similarly represented). An explanation to this fact is that polyamines induce the generation of a post-translational modification that may improve the activity of this enzyme, thus increasing the penicillin production.

Another mechanism involved in penicillin biosynthesis that is favored by polyamines is the biosynthesis of β-alanine. The amino acid β-alanine is an intermediate in pantothenic acid (vitamin B5) biosynthesis, which is converted to 4′-phosphopantetheine and subsequently, to coenzyme A. The 4′-phosphopantetheine is an essential prosthetic group for several enzymes, including the ACV synthetase, which is the first enzyme of the penicillin biosynthetic pathway [66–68]. In bacteria, pantothenic acid is synthesized by the condensation of pantoate, an intermediate in valine biosynthesis, with β-alanine, produced by the decarboxylation of L-aspartate [69,70]. In yeast, the formation of pantoate involves the same enzymatic steps as in bacteria, whereas β-alanine biosynthesis differs from that and is dependent upon polyamine biosynthesis and upon the amine oxidase encoded by the *fms1* gene [71]. Amine oxidases can degrade polyamines with the production of the aldehyde compound 3-aminopropanal [72,73], implying that further oxidation of 3-aminopropanal by an aldehyde dehydrogenase would also be required for β-alanine biosynthesis in yeast [30]. This result correlates well with the increase in the spermidine synthase (giving rise to high levels of spermidine) and with the increase in the biosynthesis of acetyl-CoA by ATP citrate lyase ACL1 and dihydrolipoamide dehydrogenase Lpd1, since β-alanine is an intermediate required for the biosynthesis of coenzyme A. These findings suggest that the biosynthesis of β-alanine is increased after the addition of these polyamines and are in agreement with previous reports suggesting that spermine, spermidine and 1,3-DAP are precursors of β-alanine in maize shoots as well as in bacteria [74,75].

Enzymes of the homogentisate pathway, which leads to the degradation of phenylacetic acid, are also clearly influenced by polyamines and could also explain the increase in penicillin

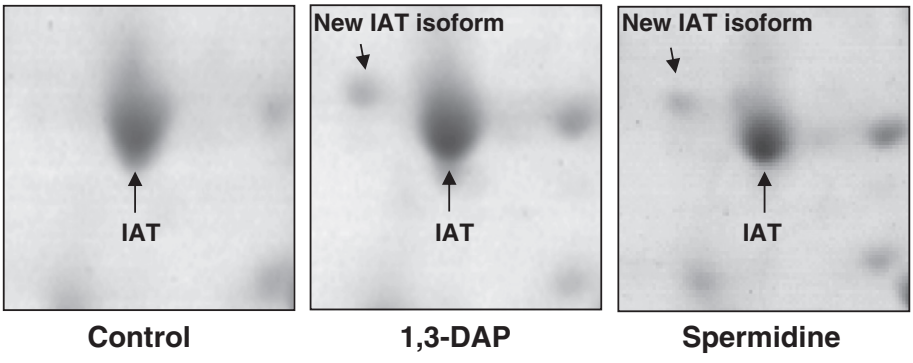

Fig. 7 – Close-up view of the new IAT isoform induced by 1,3-DAP and spermidine. Enlargement of the gel portion containing the β-subunit of IAT.

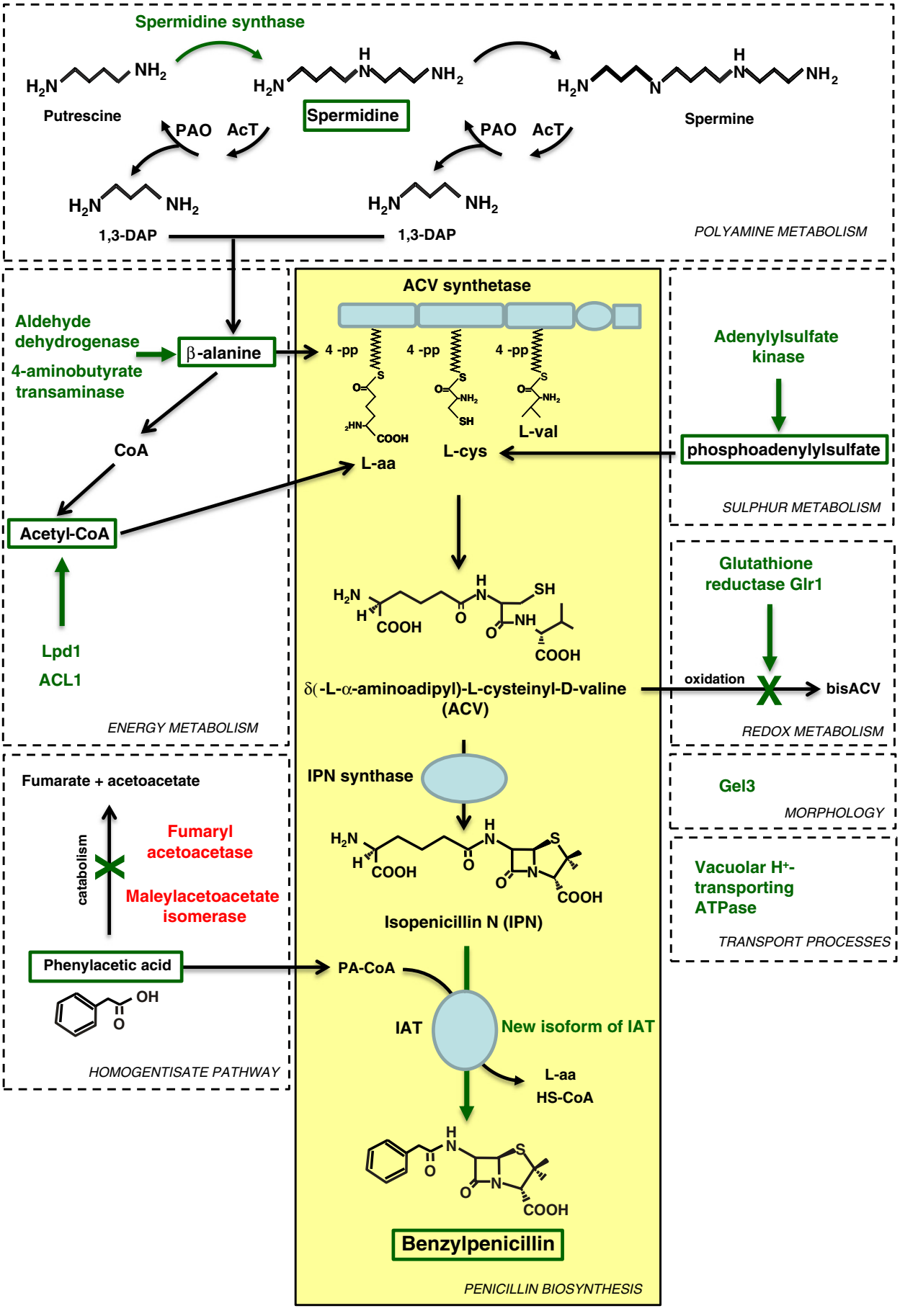
Spermidine synthase
Putrescine
Spermidine
Spermine
PAO
AcT
PAO
AcT
1,3-DAP
1,3-DAP
POLYAMINE METABOLISM
ACV synthetase
Aldehyde dehydrogenase
4-aminobutyrate transaminase
β-alanine
4 -pp
4 -pp
4 -pp
L-val
L-cys
L-aa
CoA
Acetyl-CoA
Lpd1
ACL1
ENERGY METABOLISM
δ(-L-α-aminoadipyl)-L-cysteinyl-D-valine (ACV)
Adenylylsulfate kinase
phosphoadenylylsulfate
SULPHUR METABOLISM
Glutathione reductase Glr1
oxidation
bisACV
REDOX METABOLISM
Gel3
MORPHOLOGY
Vacuolar H+-transporting ATPase
TRANSPORT PROCESSES
IPN synthase
Isopenicillin N (IPN)
Fumarate + acetoacetate
catabolism
Fumaryl acetoacetase
Maleylacetoacetate isomerase
Phenylacetic acid
HOMOGENTISATE PATHWAY
PA-CoA
IAT
New isoform of IAT
L-aa
HS-CoA
Benzylpenicillin
PENICILLIN BIOSYNTHESIS

titers. Phenylacetic acid is industrially used as the side-chain precursor for the production of benzylpenicillin in submerged fermentations. The positive influence of feeding penicillin fermentations with side chain precursors has been well-documented since the beginning of industrial penicillin production. Because of the existence of several paralogs of IAT that introduce different side chains, phenylacetic acid must be supplemented to promote the biosynthesis of benzylpenicillin rather than other natural penicillins [76]. The effectiveness of this side chain precursor is dependent on its resistance to oxidation by *P. chrysogenum* [77]. The first step of the phenylacetic acid catabolic pathway is a 2-hydroxylation by a microsomal cytochrome P450 monooxygenase, and it is well documented that modifications of this enzyme led to a reduced degradation of phenylacetic acid and to penicillin overproduction [78]. Therefore, there is a clear negative correlation between the abundance of the first enzyme of this pathway and penicillin biosynthesis. Polyamines, specially 1,3-DAP, reduced the synthesis of late enzymes of the homogentisate pathway; therefore it is likely that the increased penicillin titers observed after polyamines addition are also related to the downregulation of these late enzymes.

After the treatment with polyamines, some chaperones and foldases are induced and some repressed. The reason for this behaviour is likely due to the complexity of the interactions that occur in the endoplasmic reticulum between different chaperons and foldases and the multifunctionality of these chaperons. Thus, some of the processes in which these proteins are involved might be of benefit for the overproduction of some penicillin biosynthetic proteins, whereas other processes would negatively affect the final production, as it has been suggested for BiP or calnexin [79,80].

Although initially not related to the biosynthesis of penicillin, another common feature observed for 1,3-DAP and spermidine is that they induce the synthesis of a probable glycosylphosphatidylinositol-anchored beta(1–3)glucanosyltransferase, Gel3, which plays active roles in fungal cell wall biosynthesis and morphogenesis. The major structural component of the fungal wall is β-1,3-glucan, which is subjected to a number of downstream processing steps leading to extensive branching and crosslinking to other cell wall components [81,82]. Among the key enzymes involved in downstream processing are the β-1,3-glucanosyltransferases, a family of glycosylphosphatidylinositol-anchored glycoproteins. Therefore, there seems to be a positive correlation between the important hyphal morphological modifications induced by polyamines and the overrepresentation of this enzyme after induction.

In addition to these common mechanisms, each of these two polyamines particularly affects the biosynthesis of proteins involved in pathways indirectly related to the biosynthesis of penicillin. Examples are provided specially by spermidine, which induces the biosynthesis of a probable phosphogluconate dehydrogenase Gnd1 and a probable thiamine-phosphate pyrophosphorylase/hydroxyethylthiazole kinase. The first enzyme catalyzes an NADPH regenerating reaction in the pentose phosphate pathway. An increase in the NADPH levels has been strongly correlated to β-lactam production [83–85] and it is accepted that penicillin production in the high-producer strains constitutes a major burden on the supply of NADPH [86] (biosynthesis of 1 mol of penicillin requires 8–10 mol of NADPH). The second protein is involved in the *de novo* synthesis of thiamine [87,88] that works as a cofactor of aminotransferases. Thiamine pyrophosphate (TPP) is involved in branched-chain amino acids (valine, leucine and isoleucine) biosynthesis regulating acetolactate synthase, the rate limiting enzyme in this pathway. Therefore, increasing TPP levels would favor valine accumulation, one of the precursors of β-lactam antibiotics.

One striking result obtained with spermidine is the finding that this polyamine decreases the content of the cysteine synthase, which catalyzes one of the routes of cysteine formation, namely the conversion of serine to cysteine. The latter is one of the amino acid precursors of the tripeptide ACV and its availability greatly influences penicillin production fluxes [89]. Cysteine can also be synthesized from methionine by transsulfuration by the cystathionine beta synthase. Therefore, it seems that the spermidine-mediated decrease in the levels of cysteine synthase is not affecting the biosynthesis of penicillin (which is increased in spermidine-supplemented cultures), probably because the alternative pathway for cysteine biosynthesis provides enough amino acid precursor for the biosynthesis of ACV. The predominance of the cystathionine beta synthase in the biosynthesis of penicillin is supported by the fact that this enzyme is overrepresented in penicillin high-producing strains [19].

One example of proteins specifically induced by 1,3-DAP that may be involved in pathways indirectly related to the biosynthesis of penicillin is the vacuolar H(+)-transporting ATPase. This heteromultimeric enzyme couples the energy of ATP hydrolysis to proton transport across intracellular and plasma membranes of eukaryotic cells using the H^+ gradient to energize the transport of solutes, to maintain a constant intracellular pH, and to provide a signal for intravesicular processes [17,90]. Several carriers, such as those involved in nutrient uptake, utilize the electrochemical gradient of protons (or proton motive force) that exists across the plasma membrane to energize transport. Therefore, the transport of several nutrients and other solutes that are of relevance in penicillin biosynthesis may be favored by 1,3-DAP.

Fig. 8 – Graphic representation of the main metabolic pathways affected by 1,3-DAP and connection to the benzylpenicillin biosynthetic pathway. Those proteins upregulated by 1,3-DAP are written in green color, whereas those proteins downregulated by 1,3-DAP are indicated in red color. Those metabolic steps (catalyzed by the differentially expressed proteins) that have a positive effect on penicillin biosynthesis are represented as green arrows. Those molecules whose biosynthesis is favored by 1,3-DAP are highlighted. 4´pp: 4´-phosphopantetheine; AcL1: ATP citrate lyase; AcT: acetyl transferase; Gel3: glycosylphosphatidylinositol-anchored beta(1–3)glucanosyltransferase; IAT: isopenicillin N acyltransferase; L-aa: L-α-aminoadipic acid; L-cys: L-cysteine; Lpd1: mitochondrial precursor of dihydrolipoamide dehydrogenase; L-val: L-valine; PA-CoA: phenylacetyl-CoA; PAO: polyamine oxidase.

Another finding that may be related to this protein is the positive effect that 1,3-DAP exerts on the formation of vesicles. Cargo vesicles formed in the ER have been reported to play an important role in the biosynthesis of aflatoxins [16,17]. Interestingly, one of the enzymes found in these vesicles is spermidine synthase [91].

Another metabolic pathway that seems to be specifically favored by spermidine is the biosynthesis of porphyrins. Enzymes catalyzing different steps of the pathway, such as probable 5-aminolevulinic acid synthase HemA and a probable coproporphyrinogen oxidase III Hem13 were induced by spermidine. Porphyrins are a group of organic compounds well-known as the pigment in red blood cells and porphyrin-related pigments may be responsible, at least in part, for the intense color shown by the solid medium after growing *P. chrysogenum* treated with spermidine [8]. Since 1,3-DAP also

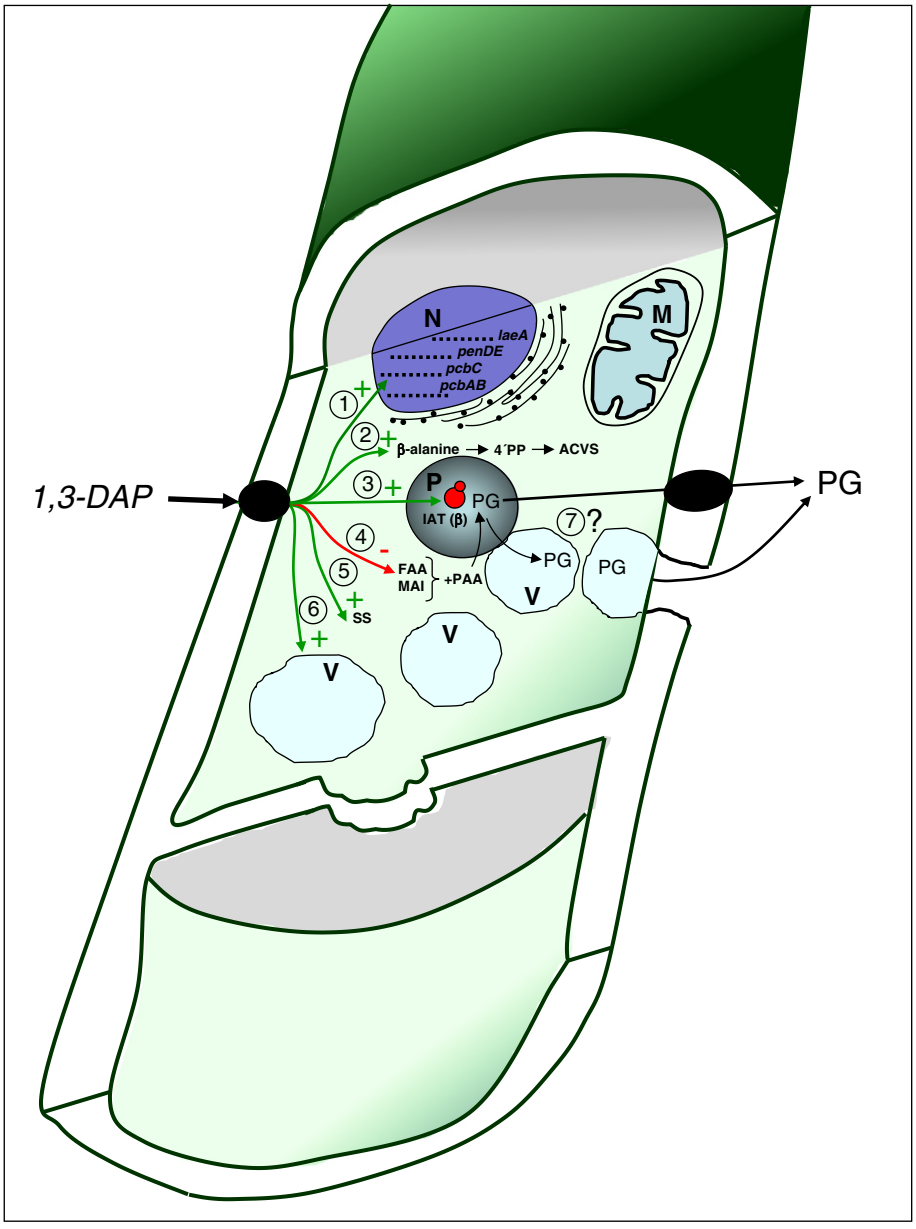

Fig. 9 – Schematic representation of some processes modified by 1,3-DAP. 1: Induction of the expression of the penicillin biosynthetic genes *pcbAB*, *pcbC* and *penDE* and the global regulator *laeA* gene. 2: Positive effect in the biosynthesis of β-alanine, an intermediate of 4´-phosphopantetheine (essential prosthetic group for ACV synthetase). 3: Induction of a new isoform of the IAT β-subunit. 4: Reduction of late enzymes of the phenylacetic acid catabolism, with a probable increase in the availability of the benzylpenicillin side chain precursor. 5: Increase in the expression of the spermidine synthase. 6: Increase in the number of vesicles. 7: Hypothetically, the increase in the number of vesicles may facilitate fusion events to peroxisomes and constitute a mechanism of benzylpenicillin secretion similar to exocytosis. 4´ PP: 4´-phosphopantetheine; ACVS: ACV synthetase; FAA: fumarylacetoacetase; IAT: Isopenicillin N acyltransferase; M: Mitochondrion; MAI: Maleylacetoacetate isomerase; N: Nucleus; P: Peroxisome; PAA: Phenylacetic acid; PG: Benzylpenicillin; SS: Spermidine synthase; V: Vesicle. This scheme has been elaborated according to the results obtained in this and in previous works [8,9].

gave rise to a more intense color but did not increase significantly the biosynthesis of porphyrins, the induction of the biosynthesis of other pigments by these polyamines cannot be ruled out.

In conclusion, we have observed that the addition of 1,3-DAP and spermidine leads to the modification of the synthesis of several enzymes involved in numerous metabolic processes. In summary, as a result of modifications in the expression of enzymes involved directly or indirectly in the biosynthesis of penicillin and precursor compounds (Fig. 8), 1,3-DAP and spermidine are responsible for an increase in the biosynthesis of the β-lactam antibiotic penicillin. These inducers, synthesized endogenously by *P. chrysogenum* act as communication signals that trigger differentiation and self-defense against competitor bacteria by increasing the biosynthesis of penicillin. Fig. 9 summarizes the main cell processes that are modified by 1,3-DAP leading to an increase in the biosynthesis and secretion of penicillin.

Acknowledgments

This work was supported by a grant of the European Union (Eurofungbase Consortium). We acknowledge the excellent technical assistance of B. Martín, J. Merino and A. Mulero (INBIOTEC, Spain).

REFERENCES

[1] Keller NP, Turner G, Bennett JW. Fungal secondary metabolism — from biochemistry to genomics. Nat Rev Microbiol 2005;3:937–47.
[2] Martín JF, Ullán RV, García-Estrada C. Regulation and compartmentalization of β-lactam biosynthesis. Microb Biotechnol 2010;3:285–99.
[3] Martín JF, Ullán RV, García-Estrada C. Role of peroxisomes in the biosynthesis and secretion of β-lactams and other secondary metabolites. J Ind Microbiol Biotechnol 2012;39:367–82.
[4] Aharonowitz Y, Cohen G, Martin JF. Penicillin and cephalosporin biosynthetic genes: structure, organization, regulation, and evolution. Annu Rev Microbiol 1992;46:461–95.
[5] Brakhage AA. Molecular regulation of beta-lactam biosynthesis in filamentous fungi. Microbiol Mol Biol Rev 1998;62:547–85.
[6] Martín JF. Molecular control of expression of penicillin biosynthesis genes in fungi: regulatory proteins interact with a bidirectional promoter region. J Bacteriol 2000;182:2355–62.
[7] Ozcengiz G, Demain AL. Recent advances in the biosynthesis of penicillins, cephalosporins and clavams and its regulation. Biotechnol Adv 2013;31:287–311.
[8] Martín J, García-Estrada C, Kosalková K, Ullán RV, Albillos SM, Martín JF. The inducers 1,3-diaminopropane and spermidine produce a drastic increase in the expression of the penicillin biosynthetic genes for prolonged time, mediated by the LaeA regulator. Fungal Genet Biol 2012;49:1004–13.
[9] Martín J, García-Estrada C, Rumbero A, Recio E, Albillos SM, Ullán RV, et al. Characterization of an autoinducer of penicillin biosynthesis in *Penicillium chrysogenum*. Appl Environ Microbiol 2011;77:5688–96.
[10] Kosalková K, García-Estrada C, Ullán RV, Godio RP, Feltrer R, Teijeira F, et al. The global regulator LaeA controls penicillin biosynthesis, pigmentation and sporulation, but not roquefortine C synthesis in *Penicillium chrysogenum*. Biochimie 2009;91:214–25.
[11] Bok JW, Keller NP. LaeA, a regulator of secondary metabolism in *Aspergillus* spp. Eukaryot Cell 2004;3:527–35.
[12] Müller WH, van der Krift TP, Krouwer AJ, Wösten HA, van der Voort LH, Smaal EB, et al. Localization of the pathway of the penicillin biosynthesis in *Penicillium chrysogenum*. EMBO J 1991;10:489–95.
[13] García-Estrada C, Vaca I, Fierro F, Sjollema K, Veenhuis M, Martín JF. The unprocessed preprotein form IATC103S of the isopenicillin N acyltransferase is transported inside peroxisomes and regulates its self-processing. Fungal Genet Biol 2008;45:1043–52.
[14] Kiel JA, van den Berg MA, Fusetti F, Poolman B, Bovenberg RA, Veenhuis M, et al. Matching the proteome to the genome: the microbody of penicillin-producing *Penicillium chrysogenum* cells. Funct Integr Genomics 2009;9:167–84.
[15] Chanda A, Roze LV, Kang S, Artymovich KA, Hicks GR, Raikhel NV, et al. A key role for vesicles in fungal secondary metabolism. Proc Natl Acad Sci U S A 2009;106:19533–8.
[16] Roze LV, Chanda A, Linz JE. Compartmentalization and molecular traffic in secondary metabolism: a new understanding of established cellular processes. Fungal Genet Biol 2011;48:35–48.
[17] Martín JF, García-Estrada C, Ullán RV. Transport of substrates into peroxisomes: the paradigm of β-lactam biosynthetic intermediates. Biomol Concepts 2013;4:197–211.
[18] Barreiro C, Martín JF, García-Estrada C. Proteomics shows new faces for the old penicillin producer *Penicillium chrysogenum*. J Biomed Biotechnol 2012;2012:105109.
[19] Jami MS, Barreiro C, García-Estrada C, Martín JF. Proteome analysis of the penicillin producer *Penicillium chrysogenum*: characterization of protein changes during the industrial strain improvement. Mol Cell Proteomics 2010;9:1182–98.
[20] Jami MS, García-Estrada C, Barreiro C, Cuadrado AA, Salehi-Najafabadi Z, Martín JF. The *Penicillium chrysogenum* extracellular proteome. Conversion from a food-rotting strain to a versatile cell factory for white biotechnology. Mol Cell Proteomics 2010;9:2729–44.
[21] Casqueiro J, Bañuelos O, Gutiérrez S, Hijarrubia MJ, Martín JF. Intrachromosomal recombination between direct repeats in *Penicillium chrysogenum*: gene conversion and deletion events. Mol Gen Genet 1999;261:994–1000.
[22] Candiano G, Bruschi M, Musante L, Santucci L, Ghiggeri GM, Carnemolla B, et al. Blue silver: a very sensitive colloidal Coomassie G-250 staining for proteome analysis. Electrophoresis 2004;25:1327–33.
[23] Sussman M, Osborn MJ. UDP-Galactose polysaccharide transferase in the cellular slime mold, *Dictyostelium discoideum*: appearance and disappearance of activity during cell differenciation. Proc Natl Acad Sci U S A 1964;52:81–7.
[24] Dimond RL, Farnsworth PA, Loomis WF. Isolation and characterization of mutations affecting UDPG pyrophosphorylase activity in *Dictyostelium discoideum*. Dev Biol 1976;50:169–81.
[25] Ragheb JA, Dottin RP. Structure and sequence of a UDP glucose pyrophosphorylase gene of *Dictyostelium discoideum*. Nucleic Acids Res 1987;15:3891–906.
[26] Jaklitsch WM, Kubicek CP. Homocitrate synthase from *Penicillium chrysogenum*. Localization, purification of the cytosolic isoenzyme, and sensitivity to lysine. Biochem J 1990;269:247–53.
[27] Bañuelos O, Casqueiro J, Steidl S, Gutiérrez S, Brakhage A, Martín JF. Subcellular localization of the homocitrate synthase in *Penicillium chrysogenum*. Mol Genet Genomics 2002;266:711–9.
[28] Devenish RJ, Prescott M, Roucou X, Nagley P. Insights into ATP synthase assembly and function through the molecular

genetic manipulation of subunits of the yeast mitochondrial enzyme complex. Biochim Biophys Acta 2000;1458:428–42.
[29] Takeda M, Chen WJ, Saltzgaber J, Douglas MG. Nuclear genes encoding the yeast mitochondrial ATPase complex. Analysis of ATP1 coding the F1-ATPase alpha-subunit and its assembly. J Biol Chem 1986;261:15126–33.
[30] White WH, Skatrud PL, Xue Z, Toyn JH. Specialization of function among aldehyde dehydrogenases: the ALD2 and ALD3 genes are required for beta-alanine biosynthesis in *Saccharomyces cerevisiae*. Genetics 2003;163:69–77.
[31] Valmaseda EM, Campoy S, Naranjo L, Casqueiro J, Martín JF. Lysine is catabolized to 2-aminoadipic acid in *Penicillium chrysogenum* by an omega-aminotransferase and to saccharopine by a lysine 2-ketoglutarate reductase. Characterization of the omega-aminotransferase. Mol Genet Genomics 2005;274:272–82.
[32] Garrett MD, Zahner JE, Cheney CM, Novick PJ. GDI1 encodes a GDP dissociation inhibitor that plays an essential role in the yeast secretory pathway. EMBO J 1994;13:1718–28.
[33] Morishima N, Nakagawa K, Yamamoto E, Shibata T. A subunit of yeast site-specific endonuclease SceI is a mitochondrial version of the 70-kDa heat shock protein. J Biol Chem 1990;265:15189–97.
[34] Van Dyke N, Baby J, Van Dyke MW. Stm1p, a ribosome-associated protein, is important for protein synthesis in *Saccharomyces cerevisiae* under nutritional stress conditions. J Mol Biol 2006;358:1023–31.
[35] Martín JF, Casqueiro J, Kosalková K, Marcos AT, Gutiérrez S. Penicillin and cephalosporin biosynthesis: mechanism of carbon catabolite regulation of penicillin production. Antonie Van Leeuwenhoek 1999;75:21–31.
[36] Yotov WV, Moreau A, St-Arnaud R. The alpha chain of the nascent polypeptide-associated complex functions as a transcriptional coactivator. Mol Cell Biol 1998;18:1303–11.
[37] Lin DT, Lechleiter JD. Mitochondrial targeted cyclophilin D protects cells from cell death by peptidyl prolyl isomerization. J Biol Chem 2002;277:31134–41.
[38] Baines CP, Kaiser RA, Purcell NH, Blair NS, Osinska H, Hambleton MA, et al. Loss of cyclophilin D reveals a critical role for mitochondrial permeability transition in cell death. Nature 2005;434:658–62.
[39] Cohen G, Argaman A, Schreiber R, Mislovati M, Aharonowitz Y. The thioredoxin system of *Penicillium chrysogenum* and its possible role in penicillin biosynthesis. J Bacteriol 1994;176: 973–84.
[40] Osterås M, Boncompagni E, Vincent N, Poggi MC, Le Rudulier D. Presence of a gene encoding choline sulfatase in *Sinorhizobium meliloti* bet operon: choline-O-sulfate is metabolized into glycine betaine. Proc Natl Acad Sci U S A 1998;95:11394–9.
[41] Bateman RL, Bhanumoorthy P, Witte JF, McClard RW, Grompe M, Timm DE. Mechanistic inferences from the crystal structure of fumarylacetoacetate hydrolase with a bound phosphorus-based inhibitor. J Biol Chem 2001;276:15284–91.
[42] Fleck CB, Brock M. Re-characterisation of *Saccharomyces cerevisiae* Ach1p: fungal CoA-transferases are involved in acetic acid detoxification. Fungal Genet Biol 2009;46: 473–85.
[43] Sheterline P, Clayton J, Sparrow JC. Actins. 3rd ed. London: Academic Press Ltd.; 1996.
[44] Iverson TM, Luna-Chavez C, Cecchini G, Rees DC. Structure of the *Escherichia coli* fumarate reductase respiratory complex. Science 1999;284:1961–6.
[45] Eggink G, Lageveen RG, Altenburg B, Witholt B. Controlled and functional expression of the *Pseudomonas oleovorans* alkane utilizing system in *Pseudomonas putida* and *Escherichia coli*. J Biol Chem 1987;262:17712–8.
[46] van Beilen JB, Panke S, Lucchini S, Franchini AG, Röthlisberger M, Witholt B. Analysis of *Pseudomonas putida* alkane-degradation gene clusters and flanking insertion sequences: evolution and regulation of the alk genes. Microbiology 2001;147:1621–30.
[47] O'connor T, Ireland LS, Harrison DJ, Hayes JD. Major differences exist in the function and tissue-specific expression of human aflatoxin B1 aldehyde reductase and the principal human aldo-keto reductase AKR1 family members. Biochem J 1999;343:487–504.
[48] Palackal NT, Burczynski ME, Harvey RG, Penning TM. Metabolic activation of polycyclic aromatic hydrocarbon trans-dihydrodiols by ubiquitously expressed aldehyde reductase (AKR1A1). Chem Biol Interact 2001;130–132:815–24.
[49] Ramos F, el Guezzar M, Grenson M, Wiame JM. Mutations affecting the enzymes involved in the utilization of 4-aminobutyric acid as nitrogen source by the yeast *Saccharomyces cerevisiae*. Eur J Biochem 1985;149:401–4.
[50] Coleman ST, Fang TK, Rovinsky SA, Turano FJ, Moye-Rowley WS. Expression of a glutamate decarboxylase homologue is required for normal oxidative stress tolerance in *Saccharomyces cerevisiae*. J Biol Chem 2001;276:244–50.
[51] Stehle T, Schulz GE. Refined structure of the complex between guanylate kinase and its substrate GMP at 2.0 A resolution. J Mol Biol 1992;224:1127–41.
[52] Seufert W, Jentsch S. Ubiquitin-conjugating enzymes UBC4 and UBC5 mediate selective degradation of short-lived and abnormal proteins. EMBO J 1990;9:543–50.
[53] Melin P, Schnürer J, Wagner EG. Characterization of *phiA*, a gene essential for phialide development in *Aspergillus nidulans*. Fungal Genet Biol 2003;40:234–41.
[54] Pegg AE, Coward JK. Growth of mammalian cells in the absence of the accumulation of spermine. Biochem Biophys Res Commun 1985;133:82–9.
[55] Pegg AE, Xiong H, Feith DJ, Shantz LM. S-adenosylmethionine decarboxylase: structure, function and regulation by polyamines. Biochem Soc Trans 1998;26:580–6.
[56] Behe M, Felsenfeld G. Effects of methylation on a synthetic polynucleotide: the B–Z transition in poly(dG-m5dC).poly(dG-m5dC). Proc Natl Acad Sci U S A 1981;78:1619–23.
[57] Pingoud A. Spermidine increases the accuracy of type II restriction endonucleases. Suppression of cleavage at degenerate, non-symmetrical sites. Eur J Biochem 1985;147: 105–9.
[58] Feuerstein BG, Williams LD, Basu HS, Marton LJ. Implications and concepts of polyamine-nucleic acid interactions. J Cell Biochem 1991;46:37–47.
[59] Hampel KJ, Crosson P, Lee JS. Polyamines favor DNA triplex formation at neutral pH. Biochemistry 1991;30:4455–9.
[60] Pegg AE, Coward JK. Effect of N-(n-butyl)-1,3-diaminopropane on polyamine metabolism, cell growth and sensitivity to chloroethylating agents. Biochem Pharmacol 1993;46:717–24.
[61] Yamada H, Kimiyasu I, Yoshiki T. Oxidation of polyamines by fungal enzymes. Agric Biol Chem 1980;44:2469–76.
[62] Barredo JL, van Solingen P, Díez B, Alvarez E, Cantoral JM, Kattevilder A, et al. Cloning and characterization of the acyl-coenzyme A: 6-aminopenicillanic-acid-acyltransferase gene of *Penicillium chrysogenum*. Gene 1989;83:291–300.
[63] Whiteman PA, Abraham EP, Baldwin JE, Fleming MD, Schofield CJ, Sutherland JD, et al. Acyl coenzyme A: 6-aminopenicillanic acid acyltransferase from *Penicillium chrysogenum* and *Aspergillus nidulans*. FEBS Lett 1990;262: 342–4.
[64] Tobin MB, Fleming MD, Skatrud PL, Miller JR. Molecular characterization of the acyl-coenzyme A: isopenicillin N acyltransferase gene (*penDE*) from *Penicillium chrysogenum* and *Aspergillus nidulans* and activity of recombinant enzyme in *Escherichia coli*. J Bacteriol 1990;172:5908–14.
[65] Tobin MB, Baldwin JE, Cole SC, Miller JR, Skatrud PL, Sutherland JD. The requirement for subunit interaction in the production *of Penicillium chrysogenum* acyl-coenzyme A:

isopenicillin N acyltransferase in *Escherichia coli*. Gene 1993;132:199–206.
[66] Baldwin JE, Bird JW, O'Callaghan NM, Schofield CJ, Willis AC. Isolation and partial characterisation of ACV synthetase from *Cephalosporium acremonium* and *Streptomyces clavuligerus*. Evidence for the presence of phosphopantothenate in ACV synthetase. J Antibiot (Tokyo) 1991;44:241–8.
[67] Aharonowitz Y, Bergmeyer J, Cantoral JM, Cohen G, Demain AL, Fink U, et al. Delta-(L-alpha-aminoadipyl)-L-cysteinyl-D-valine synthetase, the multienzyme integrating the four primary reactions in beta-lactam biosynthesis, as a model peptide synthetase. Biotechnology (NY) 1993;11:807–10.
[68] Martin JF. Alpha-aminoadipyl-cysteinyl-valine synthetases in beta-lactam producing organisms. From Abraham's discoveries to novel concepts of non-ribosomal peptide synthesis. J Antibiot (Tokyo) 2000;53:1008–21.
[69] Williamson JM, Brown GM. Purification and properties of L-Aspartate-alpha-decarboxylase, an enzyme that catalyzes the formation of beta-alanine in *Escherichia coli*. J Biol Chem 1979;254:8074–82.
[70] Jackowski S. Cell cycle regulation of membrane phospholipid metabolism. J Biol Chem 1996;271:20219–22.
[71] White WH, Gunyuzlu PL, Toyn JH. *Saccharomyces cerevisiae* is capable of de Novo pantothenic acid biosynthesis involving a novel pathway of beta-alanine production from spermine. J Biol Chem 2001;276:10794–800.
[72] Hölttä E. Oxidation of spermidine and spermine in rat liver: purification and properties of polyamine oxidase. Biochemistry 1977;16:91–100.
[73] Large PJ. Enzymes and pathways of polyamine breakdown in microorganisms. FEMS Microbiol Rev 1992;8:249–62.
[74] Razin S, Bachrach U, Gery I. Formation of beta-alanine from spermine and spermidine by *Pseudomonas aeruginosa*. Nature 1958;181:700–1.
[75] Terano S, Suzuki Y. Formation of β-alanine from spermine and spermidine in maize shoots. Phytochemistry 1978;17:148–9.
[76] Hersbach GJM, van der Beek CP, van Dijck PWM. The penicillins: properties, biosynthesis, and fermentation. In: Vandamme EJ, editor. Biotechnology of Industrial Antibiotics. New York: Marcel Dekker; 1984. p. 45–140.
[77] Hillenga DJ, Versantvoort H, van der Molen S, Driessen A, Konings WN. *Penicillium chrysogenum* takes up the penicillin g precursor phenylacetic acid by passive diffusion. Appl Environ Microbiol 1995;61:2589–95.
[78] Rodríguez-Sáiz M, Barredo JL, Moreno MA, Fernández-Cañón JM, Peñalva MA, Díez B. Reduced function of a phenylacetate-oxidizing cytochrome p450 caused strong genetic improvement in early phylogeny of penicillin-producing strains. J Bacteriol 2001;183:5465–71.
[79] Conesa A, Jeenes D, Archer DB, van den Hondel CA, Punt PJ. Calnexin overexpression increases manganese peroxidase production in *Aspergillus niger*. Appl Environ Microbiol 2002;68:846–51.
[80] Lombraña M, Moralejo FJ, Pinto R, Martín JF. Modulation of *Aspergillus awamori* thaumatin secretion by modification of *bipA* gene expression. Appl Environ Microbiol 2004;70:5145–52.
[81] Mouyna I, Fontaine T, Vai M, Monod M, Fonzi WA, Diaquin M, et al. Glycosylphosphatidylinositol-anchored glucanosyltransferases play an active role in the biosynthesis of the fungal cell wall. J Biol Chem 2000;275:14882–9.
[82] Klis FM, Mol P, Hellingwerf K, Brul S. Dynamics of cell wall structure in *Saccharomyces cerevisiae*. FEMS Microbiol Rev 2002;26:239–56.
[83] Jørgensen H, Nielsen J, Villadsen J, Møllgaard H. Metabolic flux distributions in *Penicillium chrysogenum* during fed-batch cultivations. Biotechnol Bioeng 1995;46:117–31.
[84] Henriksen CM, Christensen LH, Nielsen J, Villadsen J. Growth energetics and metabolic fluxes in continuous cultures of *Penicillium chrysogenum*. J Biotechnol 1996;45:149–64.
[85] van Gulik WM, de Laat WT, Vinke JL, Heijnen JJ. Application of metabolic flux analysis for the identification of metabolic bottlenecks in the biosynthesis of penicillin-G. Biotechnol Bioeng 2000;68:602–18.
[86] Kleijn RJ, Liu F, van Winden WA, van Gulik WM, Ras C, Heijnen JJ. Cytosolic NADPH metabolism in penicillin-G producing and non-producing chemostat cultures of *Penicillium chrysogenum*. Metab Eng 2007;9:112–23.
[87] Nosaka K, Nishimura H, Kawasaki Y, Tsujihara T, Iwashima A. Isolation and characterization of the THI6 gene encoding a bifunctional thiamin-phosphate pyrophosphorylase/hydroxyethylthiazole kinase from *Saccharomyces cerevisiae*. J Biol Chem 1994;269:30510–6.
[88] Mizote T, Tsuda M, Smith DD, Nakayama H, Nakazawa T. Cloning and characterization of the thiD/J gene of *Escherichia coli* encoding a thiamin-synthesizing bifunctional enzyme, hydroxymethylpyrimidine kinase/phosphomethylpyrimidine kinase. Microbiology 1999;145:495–501.
[89] Nasution U, van Gulik WM, Ras C, Proell A, Heijnen JJ. A metabolome study of the steady-state relation between central metabolism, amino acid biosynthesis and penicillin production in *Penicillium chrysogenum*. Metab Eng 2008;10:10–23.
[90] Nelson N, Perzov N, Cohen A, Hagai K, Padler V, Nelson H. The cellular biology of proton-motive force generation by V-ATPases. J Exp Biol 2000;203(Pt1):89–95.
[91] Linz JE, Chanda A, Hong SY, Whitten DA, Wilkerson C, Roze LV. Proteomic and biochemical evidence support a role for transport vesicles and endosomes in stress response and secondary metabolism in *Aspergillus parasiticus*. J Proteome Res 2012;11:767–75.